ARTICLE IN PRESS

Journal of Computational Physics xxx (2011) xxx–xxx

Contents lists available at SciVerse ScienceDirect

Journal of Computational Physics

journal homepage: www.elsevier.com/locate/jcp

Filtering skill for turbulent signals for a suite of nonlinear and linear extended Kalman filters

M. Branicki *, B. Gershgorin, A.J. Majda

Department of Mathematics and Center for Atmosphere and Ocean Science, Courant Institute of Mathematical Sciences, New York University, NY 10012, United States

ARTICLE INFO

Article history:
Received 26 February 2011
Received in revised form 14 October 2011
Accepted 15 October 2011
Available online xxxx

Keywords:
Filtering turbulence
Stochastic parameter estimation
Model error
Gaussian closure filter
Extended Kalman Filter
Data assimilation

ABSTRACT

The filtering skill for turbulent signals from nature is often limited by errors due to utilizing an imperfect forecast model. In particular, real-time filtering and prediction when very limited or no a posteriori analysis is possible (e.g. spread of pollutants, storm surges, tsunami detection, etc.) introduces a number of additional challenges to the problem. Here, a suite of filters implementing stochastic parameter estimation for mitigating model error through additive and multiplicative bias correction is examined on a nonlinear, exactly solvable, stochastic test model mimicking turbulent signals in regimes ranging from configurations with strongly intermittent, transient instabilities associated with positive finite-time Lyapunov exponents to laminar behavior. Stochastic Parameterization Extended Kalman Filter (SPEKF), used as a benchmark here, involves exact formulas for propagating the mean and covariance of the augmented forecast model including the unresolved parameters. The remaining filters use the same nonlinear forecast model but they introduce model error through different moment closure approximations and/or linear tangent approximation used for computing the second-order statistics of the augmented stochastic forecast model. A comprehensive study of filter performance is carried out in the presence of various moment closure errors which are enhanced by additional model errors due to incorrect parameters inducing additive and multiplicative stochastic biases. The estimation skill of the unresolved stochastic parameters is also discussed and it is shown that the linear tangent filter, despite its popularity, is completely unreliable in many turbulent regimes for both parameter estimation and filtering; moreover, regimes of filter divergence for the linear tangent filter are identified. The results presented here provide useful guidelines for filtering turbulent, high-dimensional, spatially extended systems with more general model errors, as well as for designing more skillful methods for superparameterization of unresolved intermittent processes in complex multi-scale models. They also provide unambiguous benchmarks for the capabilities of linear and nonlinear extended Kalman filters using incorrect statistics on an exactly solvable test bed with rich and realistic dynamics.

1. Introduction

A central problem in many contemporary applications in science and engineering lies in developing techniques for real-time statistical estimation of a state of a complex natural system based on partial observations and an imperfect model. This

* Corresponding author.
E-mail address: branicki@cims.nyu.edu (M. Branicki).

0021-9991/$ - see front matter © 2011 Elsevier Inc. All rights reserved.
doi:10.1016/j.jcp.2011.10.029

Please cite this article in press as: M. Branicki et al., Filtering skill for turbulent signals for a suite of nonlinear and linear extended Kalman filters, J. Comput. Phys. (2011), doi:10.1016/j.jcp.2011.10.029

process is referred to as *filtering* and is crucial for making accurate predictions of the future state of the considered system. Development of rapidly-deployable, efficient, accurate and robust filtering algorithms obviously poses a problem with significant practical impact in a number of strategic areas. Important contemporary examples include tracking and positioning systems, real-time filtering of multiscale turbulent signals for prediction of storm surges, tsunami detection, the spread of pollutants or hazardous plumes, as well as extreme weather and short term climate predictions.

A major difficulty in accurate filtering of noisy turbulent signals with many degrees of freedom is model error [59,41]; the fact that the observed signal from nature is estimated using an imperfect model where important physical processes are parameterized due to inadequate numerical resolution or incomplete physical understanding. Virtually all atmosphere, ocean, and climate models with sufficiently high resolution are turbulent dynamical systems with multiple spatio-temporal scales. Similarly, many contemporary engineering applications such as satellite orbit control [36,12], distributed power generation systems [61,62] or modern optical devices [55,53] require real-time filtering with nonlinear models.

Dealing with model error is often difficult since its exact properties are unknown in any realistic scenario. Various strategies for mitigating model error in nonlinear filtering have been developed and they roughly fall into techniques based on deterministic models, e.g., shadowing filters [31], and techniques combining stochastic models with sequential Bayesian filters. Miscellaneous approaches have been developed in the latter context; examples include particle filters [4,10,50,49,7,56], reduced order filters [26,58,16] and a myriad of ensemble Kalman filters [15,8,1,2,57,29] which draw from the classical Kalman filter framework [32,33]. Most of these techniques have their own niches of applicability but they generally suffer from the so-called "curse of dimensionality" (e.g., [6,7,56]) and/or the "curse of ensemble size" (e.g., [28,41]) when applied to complex multiscale systems; consequently, a common problem of these methods in the context of filtering high-dimensional turbulent systems is a large computational overhead necessary for a reliable operation.

Filters utilizing stochastic forecast models with 'on the fly' parameter estimation for reducing judicious model error offer a cheap and skillful alternative for filtering turbulent systems with many spatio-temporal scales [21,22,27,41,25]. Such filtering techniques employ the so-called state space augmentation (see, e.g., [11]) whereby the state vector is augmented with the uncertain model parameters and the augmented state is estimated using the forecast model (which is usually nonlinear in the augmented variables) in conjunction with observations. Typically, the associated stochastic parameterization incorporates Wiener (white noise) processes for the unresolved scales [17,18]. The Stochastic Parameter Estimation Filter (SPEKF, [21]) employs Ornstein–Uhlenbeck processes (with tunable decorrelation times) for the unresolved scales and uses exact analytical formulas for updating the prior second-order statistics of the forecast model; this improved filter has been successfully tested in a hierarchy of complex models [21,22,27,35,25]. However, other filter implementations based on the Extended Kalman Filter (EKF, [33]) and various moment closure approximations are possible within the same framework. These filters introduce additional model error through the use of incorrect statistics but are often easier to derive. It is therefore imperative, especially in the context of ongoing development of cheap filtering techniques for spatially extended turbulent systems, to compare the skill of these filters with SPEKF using a test model which allows for disentangling the following two sources of model error:

(i) *Incorrect statistics* used in the filtering algorithm due to a particular moment closure and/or tangent approximation applied to the forecast model.
(ii) *Imperfect forecast model used for filtering*. Various model errors fall into this category. Examples include forecast models which do not take into account certain physical phenomena or interactions, or parameterize important physical processes due to inadequate numerical resolution or incomplete physical understanding.

In this study we assess the performance of various linear and nonlinear filters employing both the stochastic parameter estimation and approximate statistics for filtering turbulent systems on a non-Gaussian forecast model which is capable of mimicking various prototypical phenomena while being mathematically tractable. Our nonlinear test model is derived from the system developed in [21] for filtering turbulent signals in the presence of a significant model error associated with hidden transient instabilities. Here, we focus on understanding the consequences of incorrect statistics introduced through various moment closures of the augmented forecast model on the filtering skill. An attractive feature of our test model is that, despite a quadratic nonlinearity in the augmented state variables, the path-wise solutions and second-order statistics of the system can be obtained analytically. Moreover, variation of control parameters in the test model, allows for tuning it to mimic a wide range of realistic turbulent signals; the dynamical regimes we focus on here, all with mean-stable dynamics, include: (i) regimes with plentiful transient instabilities, (ii) regimes with intermittent, large-amplitude bursts of transient instability interleaved with quiescent phases and (iii) laminar behavior. Combination of these features is crucial for our purposes since it allows for designing unambiguous tests uncovering the effects of errors due to incorrect statistics on the filtering skill without obscuring the results by other uncontrollable model errors. In order to assess robustness of the established filter skill hierarchy, effects of additional model errors are also considered under a simplifying assumption of perfect model structure whereby only uncertainties in the forecast model parameters are considered. We stress here that while this limited representation of model error is appropriate for understanding the effects of incorrect statistics on the filter performance, the reported filter hierarchy does not necessarily generalize to situations when a posteriori analysis of the forecast error variance can be carried out and the model covariance is inflated to minimize the so-called *innovation variance* (see, e.g., [34,3]) in order to reduce the forecast model error.

Please cite this article in press as: M. Branicki et al., Filtering skill for turbulent signals for a suite of nonlinear and linear extended Kalman filters, J. Comput. Phys. (2011), doi:10.1016/j.jcp.2011.10.029

Results discussed in the subsequent sections include:

(i) A comprehensive understanding of the effects of model error due to moment closure and tangent approximations on the filtering skill for a suite of linear and nonlinear extended Kalman filters implementing stochastic parameter estimation for different modes in the turbulent spectrum.
(ii) Identification of filters in our test suite providing the best and the most robust real-time estimation of hidden parameters in the forecast model for a range of turbulent modes.

Besides benchmarking the performance of the suite of filters in various turbulent regimes, these findings should be very useful in developing cheap techniques for filtering spatially extended systems involving multiple spatio-temporal scales and sparse observations [23–25,27,35], and for superparameterization of complex multi-scale systems [45,47] which requires blending large-scale model dynamics with simplified, yet statistically accurate, models representing unresolved turbulent processes and their intermittent interaction with the resolved large-scale dynamics.

The analysis presented here is structured as follows: The model and its different dynamical regimes mimicking turbulent signals are discussed in Section 2. The suite of filters utilizing stochastic parameter estimation through the state space augmentation and different moment closure approximations are discussed in Section 3. The skill of the filtering algorithms, as well as the effects of different sources of model error, are discussed in Sections 5, 6, 7, 7.2.1, 8, 8.2.1,9. Finally, Section 10 contains the concluding discussion and describes future goals for research in this topic.

2. The test model and its diverse regimes of mean-stable dynamics

The nonlinear forecast model for the augmented state (u,b,γ) used here for filtering a single Fourier mode of a turbulent signal is given by the following stochastic system [21,22]

$$\left.\begin{aligned} &(a)\quad \mathrm{d}u(t) = [(-\gamma(t)+i\omega)u(t)+b(t)+f(t)]\mathrm{d}t+\sigma_u \mathrm{d}W_u(t),\\ &(b)\quad \mathrm{d}b(t) = [(-\gamma_b+i\omega_b)(b(t)-\hat{b})]\mathrm{d}t+\sigma_b \mathrm{d}W_b(t),\\ &(c)\quad \mathrm{d}\gamma(t) = -d_\gamma(\gamma(t)-\hat{\gamma})\mathrm{d}t+\sigma_\gamma \mathrm{d}W_\gamma(t), \end{aligned}\right\} \tag{1}$$

where W_u, W_b are independent complex Wiener processes and W_γ is a real Wiener process. There are nine parameters in the system (1): two damping parameters γ_b, $d_\gamma > 0$, two oscillation frequencies ω and ω_b, two stationary mean terms $\hat{b}$ and $\hat{\gamma}$ and noise amplitudes σ_u, σ_b, $\sigma_\gamma > 0$; f is a deterministic forcing.

Here, we regard $u(t)$ as representing one of the resolved modes in a turbulent signal where the nonlinear mode-interaction terms are replaced by a (multiplicative) stochastic drag $\gamma(t)$ and an additive colored noise term $b(t)$, as is often done in turbulence models [39,40,13,42–44,46]. The augmented system (1) has a quadratic nonlinearity $\gamma(t)u(t)$ and was introduced in [21] for filtering multiscale turbulent signals with hidden instabilities. The stochastic parameters (or bias correction terms), $\gamma(t)$ and $b(t)$, are estimated 'on the fly' using the forecast model in conjunction with observations in order to improve the filtering skill of $u(t)$. The novel feature of this approach is that the augmented dynamics of the hidden bias correction terms (1b,c) is modelled via Ornstein–Uhlenbeck processes with finite decorrelation times, rather than constant or Wiener processes [17,18].

The nonlinear augmented system (1) has a number of attractive properties as a test model in our analysis. Firstly, the system (1) has a surprisingly reach dynamics mimicking turbulent signals in various regimes of the turbulent spectrum, including intermittently positive finite-time Lyapunov exponents, as discussed in Section 2.1. Secondly, due to the particular structure of the nonlinearity in (1), exact path-wise solutions and exact second-order statistics of this non-Gaussian system can be obtained analytically, as discussed in [23,24,21] and recapitulated in (A). The mathematical tractability of this model and its rich dynamical behavior provides a perfect test bed for analyzing effects of errors due to various moment closure approximations in a suite of filters introduced in Section 3.

2.1. Regimes of mean stable dynamics

We describe here the most interesting dynamical regimes of the system (1). All of the dynamical regimes discussed here are characterized by the mean-stability of their solutions in the sense defined below (see also (A)):

Definition 1 (*Global mean stability*). Given the solutions

$$\boldsymbol{x}(t,t_0) = (u(t,t_0), b(t,t_0), \gamma(t,t_0))^T$$

of the system (1) with initial condition for the augmented state $x_0 \equiv (u_0,b_0,\gamma_0)^T$, the dynamics of (1) is said to be globally *mean stable* if there exists a finite constant, C, depending on x_0 and t_0 such that

$$\max_{t\in[t_0,\infty)} |\overline{\boldsymbol{x}(t,t_0)}| < C,$$

for all times t_0; the overbar here and below denotes ensemble average.

Please cite this article in press as: M. Branicki et al., Filtering skill for turbulent signals for a suite of nonlinear and linear extended Kalman filters, J. Comput. Phys. (2011), doi:10.1016/j.jcp.2011.10.029

Proposition 1 (*Mean stability of system (1)*). *The dynamics of the stochastic system (1) is mean stable provided that*

$$\chi = -\hat{\gamma} + \frac{\sigma_\gamma^2}{2d_\gamma^2} < 0, \tag{2}$$

where $\hat{\gamma}$ is the mean damping in $u(t)$, d_γ is the damping in $\gamma(t)$, and σ_γ is the noise variance in (1c).

Remark. The mean stability of the system (1) is controlled by the mean damping, $\hat{\gamma}$, in $u(t)$ and the dynamical properties of fluctuations about the mean damping represented by $\gamma(t)$. The additive noise term, $b(t)$, has no effect on the mean stability of the system (1).

A simple proof of Proposition 1 is given in (A). The proof exploits the exact formulas for the first moments of (1) and does not rely on the linearization of (1).

Definition 2 (*Decorrelation time*). Since we study only one Fourier mode here, we define the decorrelation time of fluctuations in each component of (1) as the time it takes for that component to decorrelate in the statistical steady state on the attractor. Mathematically, the decorrelation time of fluctuations in scalar solution $x(t)$ is defined as the integral on the positive half-line (from 0 to ∞) of the absolute value of the autocovariance function (on the attractor)

$$\mathcal{R}(t,\tau) \equiv \overline{(x(t) - \overline{x(t)})(x(t+\tau) - \overline{x(t+\tau)})^*},$$

where the overbar denotes the ensemble average and "*" is the complex conjugate.

Using Definition 2 and the path-wise solutions of the system (1) given in (A), it is straightforward to check that the decorrelation time of fluctuations in $\gamma(t)$ is given by $1/d_\gamma$, and $1/\gamma_b$ for $b(t)$. Computation of the decorrelation time of fluctuations in $u(t)$ is more involved and not necessary for our purposes; it is sufficient here to use the approximate decorrelation time, $1/\hat{\gamma}$, based on the mean damping in $u(t)$.

Based on the mean-stability criterion (2), it is possible to distinguish the following:

Regimes of mean-stable dynamics of the system (1).

(I) $\sigma_\gamma, d_\gamma \gg 1, \sigma_\gamma/d_\gamma \sim \mathcal{O}(1)$ and $\hat{\gamma} > 0$ sufficiently large so that $\chi < 0$.
This is a regime of rapidly decorrelating $\gamma(t)$. The dynamics of $u(t)$ is dominated by frequent, short-lasting transient instabilities (see Figs. 1 and 2). Decorrelation time of fluctuations in $u(t)$ is approximately $1/\hat{\gamma}$ and can vary widely. This type of dynamics is characteristic of the turbulent energy transfer range.

(II) $\sigma_\gamma, d_\gamma \sim \mathcal{O}(1)$ small, $\sigma_\gamma/d_\gamma \sim \mathcal{O}(1)$ and $\hat{\gamma} > 0$ sufficiently large so that $\chi < 0$.
In this regime the decorrelation time of $\gamma(t)$ is long. The dynamics of $u(t)$ is characterized by intermittent bursts of large-amplitude, transient instabilities followed by quiescent phases (see Fig. 8). This regime is characteristic of the turbulent modes in the dissipative range. Similarly to (I), decorrelation time of fluctuations in $u(t)$ can vary widely in this regime.

(III) $\sigma_\gamma^2/2d_\gamma^2 \gg 1$, $\sigma_\gamma \sim \mathcal{O}(1)$ and $\hat{\gamma} \gg 1$sufficiently large so that $\chi < 0$. This regime is characteristic of the laminar modes in the turbulent spectrum (see Fig. 17). Here, fluctuations in $u(t)$ decorrelate rapidly compared to $\gamma(t)$ and the transient instabilities occur very rarely. In the extreme case when $\hat{\gamma} \gg \sigma_\gamma^2/2d_\gamma^2$ there are almost surely no transient instabilities in the dynamics of $u(t)$.

3. Suite of filters

We focus here on computationally cheap algorithms for filtering turbulent signals with multiple spatio-temporal scales which employ stochastic turbulence models for the unresolved scales. As pointed out in Section 2, the augmented stochastic forecast model (1)for filtering individual Fourier modes of the physical system is nonlinear in the augmented state variables (u, b, γ). A standard technique for estimating the the observed physical variable $u(t)$ in conjunction with the hidden stochastic parameters, γ and b, involves the linear tangent approximation of the augmented forecast model and Kalman filtering. However, the use of the classical Extended Kalman Filter (EKF, [33]) is rarely justified in practice and it often leads to divergent solutions for turbulent signals, as will be shown in Sections 7, 7.2.1, 8, 8.2.1,9.

One alternative approach to this problem, besides deriving exact model statistics as in SPEKF below, is to avoid the linearization in propagating the prior statistics in the filter through a moment closure approximation applied to the nonlinear augmented forecast model. Despite the relative simplicity of filters obtained in this way, they are not uniquely optimal in the same sense as is Kalman filtering for linear systems. One potential deficiency, common to all nonlinear extensions of the Kalman filter, is that the filter update rules only involve the second-order statistics. The Gaussianity of the signal is generally

Please cite this article in press as: M. Branicki et al., Filtering skill for turbulent signals for a suite of nonlinear and linear extended Kalman filters, J. Comput. Phys. (2011), doi:10.1016/j.jcp.2011.10.029

lost due to the nonlinearity and such filters may not be optimal anymore. Moreover, if the moment closures are used in derivation of the second-order statistics in the nonlinear filters, additional model error is introduced into the problem. It is worth remarking here that particle filters have been shown to accurately estimate higher order statistics in low-dimensional nonlinear problems. However, as already noted in the Introduction, the authors are not aware of particle filtering techniques which are practically skillful for high-dimensional problems due to the 'curse of dimensionality' [6,56,38]; a much needed progress in this area is a subject of ongoing research (see, e.g., [48, Chapter 15] and references therein).

In this section we first outline the properties of basic Kalman filtering with a linear tangent approximation which leads to the classical Tangent Extended Kalman Filter (TEKF). We then develop a general framework for filtering with quadratic models which allows us to discuss in a unified fashion four nonlinear filters based on different moment closure approximations of the augmented nonlinear forecast model (1). These four imperfect filters have long been known in the engineering literature, as discussed below. The 'youngest' member of the suite, the Stochastic Parameterization Extended Kalman Filter (SPEKF), used as a benchmark and a perfect filter in this study, exploits the particular structure of the forecast model (1) and uses exact formulas for the second-order statistics without any moment closures. The imperfect filters based on moment closures introduce additional model error but are often easier to implement. Performance of these filters and the effects of various model errors are tested and discussed in the subsequent Sections 7, 7.2.1, 8, 8.2.1,9.

3.1. Basic filtering for linear models

The classical discrete Kalman filter [32] is a two-step, predictor–corrector method which incorporates noisy observations of a physical system at a discrete sequence of times, $T_M = \{t_1, t_2, \ldots, t_M\}$, in order to adjust the model prediction for the state of the system at the same times T_M. In its original formulation the model dynamics is described by a linear stochastic process, all uncertainties and initial conditions have Gaussian distributions, and the filtering process can be described uniquely in terms of the mean state and the covariance matrix. In such a case the model forecast, $\{\boldsymbol{x}_m\}_{m=1,\ldots,M}$, and the observations, $\{\boldsymbol{v}_m\}_{m=1,\ldots,M}$, both recorded at the same sequence of times T_M can be written as:

$$\textit{model forecast}: \quad \boldsymbol{x}_{m+1} = F_{m+1}\boldsymbol{x}_m + \Phi_{m+1} + \boldsymbol{\sigma}_{m+1}, \tag{3}$$

$$\textit{observation}: \quad \boldsymbol{v}_{m+1} = G\boldsymbol{x}_{m+1} + \boldsymbol{q}_{m+1}, \tag{4}$$

where $\boldsymbol{x}_{m+1} \in \mathbb{R}^n$ represents the n-dimensional (augmented) state of the system at time t_{m+1}, F_{m+1} is a linear deterministic operator that maps $\boldsymbol{x}_m$ forward in time, Φ_{m+1} is the deterministic forcing at t_{m+1}, and $\boldsymbol{\sigma}_{m+1}$ is an n-dimensional white Gaussian vector with variance Σ_{m+1} at time t_{m+1}. For simplicity in exposition the observations $\{\boldsymbol{v}_m\}_{m=1,\ldots,M}$ of the true state are modelled here by a linear transformation with the *observation operator* G and additive white Gaussian noise $\{\boldsymbol{q}_m\}_{m=1,\ldots,M}$ with variance Q_m at time t_m.

The Kalman solution to filtering the linear system (3), (4) at the discrete sequence of times T_M produces an optimal estimate (see [32]) of the *posterior* mean and covariance of the system state at t_{m+1} based on the observation $\boldsymbol{v}_{m+1}$ and the model prediction prior to incorporating the observation. The prior mean and covariance at time t_{m+1} are denoted by $\bar{\boldsymbol{x}}_{m+1|m}$ and $R_{m+1|m}$, while the posterior mean and covariance are denoted by $\bar{\boldsymbol{x}}_{m+1|m+1}$ and $R_{m+1|m+1}$.

The second order statistics in the Kalman filter is updated iteratively as follows:

Initialization:

$$\bar{\boldsymbol{x}}_{0|0} = E[\boldsymbol{x}_0], \quad R_{0|0} = Cov[\boldsymbol{x}_0] \equiv \overline{\boldsymbol{x}_0\boldsymbol{x}_0^T}, \tag{5}$$

Prior update (model forecast):

$$\bar{\boldsymbol{x}}_{m+1|m} = F_{m+1}\bar{\boldsymbol{x}}_{m|m} + \Phi_{m+1}, \tag{6}$$

$$R_{m+1|m} = F_{m+1}R_{m|m}F_{m+1}^* + \Sigma_{m+1}. \tag{7}$$

Posterior update (observation incorporated):

$$\bar{\boldsymbol{x}}_{m+1|m+1} = \bar{\boldsymbol{x}}_{m+1|m} + K_{m+1}(\boldsymbol{v}_{m+1} - G\bar{\boldsymbol{x}}_{m+1|m}), \tag{8}$$

$$R_{m+1|m+1} = (\mathcal{I} - K_{m+1}G)R_{m+1|m}, \tag{9}$$

$$K_{m+1} = R_{m+1|m}G^*(GR_{m+1|m}G^* + Q_{m+1})^{-1}. \tag{10}$$

The operator K_{m+1} is referred to as the Kalman gain at t_{m+1} and the asterisk, "$*$" in (7) and (10) denotes the complex conjugate.

3.1.1. Tangent EKF

The procedure described below is the simplest and historically the earliest extension of the Kalman filter aimed at dealing with nonlinear stochastic forecast models (see [33]). We will refer to such a procedure as the Tangent Extended Kalman Filter (TEKF) in order to differentiate it from other extensions of the Kalman filter to nonlinear models discussed in the next section.

Please cite this article in press as: M. Branicki et al., Filtering skill for turbulent signals for a suite of nonlinear and linear extended Kalman filters, J. Comput. Phys. (2011), doi:10.1016/j.jcp.2011.10.029

Assume that the continuous-time, imperfect forecast model for the dynamics of a physical system is given by the following nonlinear (Ito) stochastic differential equation (see, e.g., [19,30])

$$\mathrm{d}\boldsymbol{x} = \boldsymbol{f}(\boldsymbol{x},t)\mathrm{d}t + \mathrm{d}\mathbf{W}(t), \quad \mathbf{W}(t) \sim \mathcal{N}_n(0,\Sigma(t)), \tag{11}$$

where $\boldsymbol{x}$ is the n-dimensional augmented state vector $\boldsymbol{x} = (\boldsymbol{x}_R, \boldsymbol{x}_H)^T$ with $\boldsymbol{x}_R$ the resolved variables and $\boldsymbol{x}_H$ the hidden stochastic parameters; $\boldsymbol{f}$ denotes the deterministic part of the augmented model (including the deterministic part of the modelled dynamics for the stochastic parameters), and $\mathbf{W}(t)$ is an n-dimensional Wiener process with covariance Σ. The stochastic noise accounts for additional unresolved processes in the forecast model, affecting both the resolved variables and the dynamics of augmented the stochastic parameters. The sequence of observations, $\{\boldsymbol{v}_m\}_{m=1,\ldots,M}$, where each $\boldsymbol{v}_m$ is a k-dimensional vector ($k \leqslant n$), is modelled here for simplicity by a linear transformation

$$\boldsymbol{v}_m = G\boldsymbol{x}_m + \mathbf{V}(t_m), \quad \mathbf{V}(t) \sim \mathcal{N}_k(0,Q(t)), \tag{12}$$

where the operator G is such that only the resolved variables are observed (i.e. $\boldsymbol{x}_H \in \ker G$) and $\mathbf{V}(t)$ is a k-dimensional ($k = n - \dim(\ker G)$) white Gaussian vector with covariance $Q(t)$.

The model forecast step in TEKF algorithm is obtained by linearizing the deterministic part of the augmented model, $\boldsymbol{f}(\boldsymbol{x},t)$, about the posterior mean $\bar{\boldsymbol{x}}_{m|m}$ at t_m and integrating the resulting tangent model between the successive observations, leading to the prior estimates $\bar{\boldsymbol{x}}_{m+1|m}, R_{m+1|m}$ at $t_{m+1} = t_m + \Delta t^{obs}$. Consequently, the forecast step in TEKF follows (6)–(10) with

$$F_{m+1} = e^{A_{m|m}\Delta t^{obs}}, \tag{13}$$

$$R_{m+1|m} = e^{A_{m|m}\Delta t^{obs}}\left(R_{m|m} + \int_{t_m}^{t_{m+1}} e^{-A_{m|m}s}\Sigma(s)e^{-A_{m|m}^T s}\mathrm{d}s\right)e^{A_{m|m}^T\Delta t^{obs}}, \tag{14}$$

where $A_{m|m} = \nabla\boldsymbol{f}(\bar{\boldsymbol{x}}_{m|m})$ is the the Jacobian of $\boldsymbol{f}$ at t_m evaluated at the posterior mean $\bar{\boldsymbol{x}}_{m|m}$. Clearly, TEKF is a discrete time priors - discrete time update filter, since both the model input and observations are incorporated at the discrete sequence of times T_M. Details of implementation of this filter for the forecast model (1) are discussed in (B.1).

3.2. Nonlinear filters for quadratic models

We introduce here a general system describing the evolution of the first two moments of the stochastic system (11) which provide an unambiguous setting for deriving extensions of the Kalman filter to nonlinear forecast models through various moment closure approximations. The discussion is restricted here to quadratic models, such as the system (1), but this framework readily generalizes to any finite dimension.

To this end, consider an imperfect quadratic forecast model (11) with the deterministic part, $\boldsymbol{f}$, in the form

$$\boldsymbol{f}(\boldsymbol{x},t) = \widehat{L}(t)\boldsymbol{x} + \mathbf{B}(\boldsymbol{x},\boldsymbol{x},t) + \overline{\mathbf{F}}(t), \tag{15}$$

where $\boldsymbol{x}$ is an n-dimensional augmented state vector, $\widehat{L}$ is a linear operator, $\mathbf{B}$ is a bilinear function, and $\overline{\mathbf{F}}$ is a deterministic forcing. In what follows we will skip the explicit dependence on time in $\boldsymbol{f}$ in order to simplify the notation.

It can be easily shown (e.g., [30]) that by adopting an analogue of the averaged Reynolds decomposition of the state vector, $\boldsymbol{x} = \bar{\boldsymbol{x}} + \boldsymbol{x}'$, such that $\overline{\boldsymbol{x}'} = 0$ and $\overline{x_i'x_j'} = 0$, the evolution of the mean $\bar{\boldsymbol{x}}$ and covariance $R \equiv \overline{\boldsymbol{x}'\boldsymbol{x}'^T}$ of the process $\boldsymbol{x}$ satisfying (11) is given by

$$\begin{cases} (a) \quad \dot{\bar{\boldsymbol{x}}} = \boldsymbol{f}(\bar{\boldsymbol{x}}) + \overline{\mathbf{B}(\boldsymbol{x}',\boldsymbol{x}')}, \\ (b) \quad \dot{R} = RA^T(\bar{\boldsymbol{x}}) + A(\bar{\boldsymbol{x}})R + \Sigma + \overline{\boldsymbol{x}'\mathbf{B}^T(\boldsymbol{x}',\boldsymbol{x}') + \mathbf{B}(\boldsymbol{x}',\boldsymbol{x}')\boldsymbol{x}'^T}, \end{cases} \tag{16}$$

where A is the Jacobian of $\boldsymbol{f}$ evaluated at $\bar{\boldsymbol{x}}$, i.e., $A(\bar{\boldsymbol{x}}) \equiv \nabla\boldsymbol{f}(\bar{\boldsymbol{x}})$ and the overbar denotes an ensemble average.

For a general quadratic forecast model, solving the Eqs. (16) requires the knowledge of the probability density $p(\boldsymbol{x},t)$ associated with the process $\boldsymbol{x}$ satisfying (11). If $p(\boldsymbol{x},t)$ is unknown, some type of moment closure is usually required. In our framework this is equivalent to making certain assumptions in (16) about the terms

$$\overline{\mathbf{B}(\boldsymbol{x}',\boldsymbol{x}')} \quad \text{and} \quad \overline{\boldsymbol{x}'\mathbf{B}^T(\boldsymbol{x}',\boldsymbol{x}') + \mathbf{B}(\boldsymbol{x}',\boldsymbol{x}')\boldsymbol{x}'^T},$$

which include, respectively, the second and third moments of the fluctuations. It is crucial to understand when these errors are important and which of the moment closures are the most sensitive to additional model errors, leading to amplified degradation of filter performance. A very attractive feature of the test model (1) is that its mean and covariance can be derived exactly due to the particular form of nonlinearity; in Sections 6, 7, 7.2.1, 8, 8.2.1,9 we will argue that this property allows for unambiguous analysis of the effects of incorrect statistics on the filter performance.

Below we introduce four nonlinear filters which will be compared with the linear filter, TEKF, in the subsequent sections. All of these filters, except for SPEKF discussed first, introduce additional model error due to various moment closure approximations applied to (16).

Please cite this article in press as: M. Branicki et al., Filtering skill for turbulent signals for a suite of nonlinear and linear extended Kalman filters, J. Comput. Phys. (2011), doi:10.1016/j.jcp.2011.10.029

3.2.1. Stochastic Parameterization Kalman Filter (SPEKF)

This filter was extensively discussed in [21,22,27]. SPEKF combines the classical Kalman steps (6)–(10) with exact formulas for the second-order statistics including the augmented stochastic parameters with no moment closure approximations. The exact analytical formulas for the mean and covariance in SPEKF were derived in [21]; they can be found due to the particular structure of the quadratic nonlinearity in the forecast model (1).

Remark. Given the true statistics of (1) at time t_m, SPEKF correctly propagates the prior mean and covariance of (1) to any future observation time t_{m+1}. If the mean and covariance at t_m are given by the posterior statistics estimated from Kalman filtering, SPEKF propagates these statistics using correct formulas but the updated prior statistics at t_{m+1} is generally different from the true statistics of (1) at t_{m+1}. This is due to the fact that Kalman filtering does not take into account the effects of higher order moments on the posterior mean and covariance when the observations are incorporated.

3.2.2. Gaussian Closure Filter (GCF)

The quasi-Gaussian closure approximation (e.g., [30]) implies neglecting the third and higher moments of the probability density $p(\boldsymbol{x},t)$ associated with the process $\boldsymbol{x}$ satisfying (11). For quadratic models only the third moments have to be neglected in (16b), i.e., GCF assumes

$$\overline{\boldsymbol{x}'\mathbf{B}^T(\boldsymbol{x}',\boldsymbol{x}')+\mathbf{B}(\boldsymbol{x}',\boldsymbol{x}')\boldsymbol{x}'^T}=0. \tag{17}$$

The closure (17) results in a fully coupled dynamical system for the second-order statistics given by

$$\begin{cases}\dot{\bar{\boldsymbol{x}}}=\boldsymbol{f}(\bar{\boldsymbol{x}})+\overline{\mathbf{B}(\boldsymbol{x}',\boldsymbol{x}')},\\ \dot{R}=RA^T(\bar{\boldsymbol{x}})+A(\bar{\boldsymbol{x}})R+\Sigma,\quad A(\bar{\boldsymbol{x}})=\nabla\boldsymbol{f}(\bar{\boldsymbol{x}}).\end{cases} \tag{18}$$

The system (18) represents the exact evolution of the second order statistics for any Gaussian process where (17) is satisfied identically. Otherwise, this closure introduces additional error into the filtering procedure.

GCF is a continuous time priors - discrete time update filter. In GCF the prior mean and covariance, $\bar{\boldsymbol{x}}_{m+1|m}, R_{m+1|m}$, are given by the solution of (18) evaluated at t_{m+1} with the initial condition: $\bar{\boldsymbol{x}}_{t_m}=\boldsymbol{x}_{m|m}, R_{t_m}=R_{m|m}$. The posterior analysis at each observation time t_m is carried out in the same way as for the Kalman filter using Eqs. (8)–(10). Details of implementation of GCF on the quadratic test model (1) are discussed in (B.4).

3.2.3. Deterministic Mean Filter (DMF)

In the engineering literature this algorithm and the tangent approximation leading to TEKF (see Section 3.1.1) are referred to, rather confusingly, as the Extended Kalman Filter (e.g., [60,53,54,14]), or as the continuous-discrete Extended Kalman Filter [52,20]. We refer to the algorithm below as DMF in order to avoid the confusion with TEKF.

Similarly to GCF, DMF is a continuous time priors - discrete time update filter. The prior mean and covariance, $\bar{\boldsymbol{x}}_{m+1|m}, R_{m+1|m}$, in DMF are updated by solving

$$\begin{cases}(a)\quad \dot{\bar{\boldsymbol{x}}}=\boldsymbol{f}(\bar{\boldsymbol{x}}),\\ (b)\quad \dot{R}=RA^T(\bar{\boldsymbol{x}})+A(\bar{\boldsymbol{x}})R+\Sigma,\quad A(\bar{\boldsymbol{x}})\equiv\nabla\boldsymbol{f}(\bar{\boldsymbol{x}}),\end{cases} \tag{19}$$

on the time interval $[t_m,t_{m+1}]$ with initial conditions $\boldsymbol{x}(t_m)=\boldsymbol{x}_{m|m}$,$R(t_m)=R_{m|m}$. The posterior analysis at each discrete observation time t_m is carried out as for the Kalman filter using Eqs. (8)–(10).

Similarly to GCF, DMF neglects the third and higher moments in the evolution of the covariance. However, DMF uses only the *deterministic* (nonlinear) part of the forecast model (11) to propagate the mean, effectively neglecting correlations between variables by assuming that

$$\overline{\boldsymbol{f}(\boldsymbol{x})}=\boldsymbol{f}(\bar{\boldsymbol{x}}),$$

which holds exactly only when $\boldsymbol{f}$ is linear. Within the general framework for quadratic models (16) this ad hoc closure corresponds to imposing

$$\overline{\boldsymbol{x}'\mathbf{B}^T(\boldsymbol{x}',\boldsymbol{x}')+\mathbf{B}(\boldsymbol{x}',\boldsymbol{x}')\boldsymbol{x}'^T}=0,\quad\text{and}\quad\overline{\mathbf{B}(\boldsymbol{x}',\boldsymbol{x}')}=0, \tag{20}$$

in the equations for the evolution of the prior mean and covariance $\bar{\boldsymbol{x}}_{m+1|m}$ and covariance $R_{m+1|m}$

Remark. (i) The ad hoc moment closure in (19), assuming that the second moments in the equation for the mean (19a) vanish, is inconsistent with the nontrivial evolution of the covariance in (19b). (ii) The covariance in DMF and GCF satisfies the same evolution equation. However, in GCF the equations for the mean and covariance are coupled through the second moments and the Jacobian, $A(\bar{\boldsymbol{x}})$, in GCF is evaluated at a different mean.

The posterior update in DMF, incorporating observations at t_{m+1}, is carried out in the same fashion as in the Kalman filter (cf. (8)–(10)). Details of the implementation of DMF on the test model (1) are discussed in (B.2).

Please cite this article in press as: M. Branicki et al., Filtering skill for turbulent signals for a suite of nonlinear and linear extended Kalman filters, J. Comput. Phys. (2011), doi:10.1016/j.jcp.2011.10.029

3.2.4. Split Deterministic Mean Filter (SDMF)

This filter uses the same moment closures as DMF but it uses the tangent approximation (like TEKF), evaluated at the discrete observation times, to update the prior covariances.

Similarly to DMF, the prior mean, $\bar{\boldsymbol{x}}_{m+1|m}$, in SDMF is updated through the deterministic (and generally nonlinear) part of the forecast model by solving

$$\dot{\bar{\boldsymbol{x}}} = \boldsymbol{f}(\bar{\boldsymbol{x}}), \tag{21}$$

on a time interval $[t_m, t_{m+1}]$ with initial condition $\boldsymbol{x}(t_m) = \bar{\boldsymbol{x}}_{m|m}$.The prior estimate of the covariance matrix, $R_{m+1|m}$, at t_{m+1} is computed, as in TEKF, by integrating (19b) between successive observations with the Jacobian $A(\bar{\boldsymbol{x}})$ evaluated at $\bar{\boldsymbol{x}}_{m|m}$, i.e.,

$$R_{m+1|m} = e^{A_{m|m}\Delta t^{obs}}\left(R_{m|m} + \int_{t_m}^{t_{m+1}} e^{-A_{m|m}s}\Sigma(s)e^{-A_{m|m}^T s}\mathrm{d}s\right)e^{A_{m|m}^T \Delta t^{obs}}, \tag{22}$$

where

$$A_{m|m} = \nabla \boldsymbol{f}(\bar{\boldsymbol{x}}_{m|m}), \quad \Delta t^{obs} = t_{m+1} - t_m. \tag{23}$$

The posterior update is carried out as in the Kalman filter through (8)–(10). Details of implementation of SDMF on the test model (1) are discussed in (B.3).

4. Generation of the synthetic "truth" signal

As already mentioned earlier, our main focus here is to understand the effects of incorrect statistics used in the filters employing stochastic parameter estimation on the filter performance. In order to avoid overshadowing these errors by various other uncontrollable model errors, we use the same system (1) to generate the synthetic truth and for filtering the observed signal. The true system parameters are denoted by

$$\Lambda = \{\omega, \sigma_u, \quad \hat{\gamma}, d_\gamma, \sigma_\gamma, \quad \hat{b}, \gamma_b, \omega_b, \sigma_b\}, \tag{24}$$

while the system parameters used for filtering the observed signal are

$$\Lambda^M = \left\{\omega^M, \sigma_u^M, \quad \hat{\gamma}^M, d_\gamma^M, \sigma_\gamma^M, \quad \hat{b}^M, \gamma_b^M, \omega_b^M, \sigma_b^M\right\}. \tag{25}$$

The parameter set Λ^M used for filtering is, in principle, independent of the parameters Λ used for generating the truth; when $\Lambda^M = \Lambda$ the imperfect filters are only affected by the errors due to incorrect statistics. The numerical realizations of the truth signal are obtained by integrating the exact solutions (A.1)–(A.3) of (1) which are derived in (A).

We assume that only the 'resolved' variable $u(t)$ is directly observed. The augmented dynamics of the hidden variables in (1), γ and b, is estimated adaptively during the filtering from the observations of $u(t)$ and from the forecast model. Consequently, the observation operator G used in the posterior update (8)–(10) in all filters has the form

$$\widehat{G} = \begin{pmatrix} 1 & 0 & 0 & 0 & 0 \\ 0 & 1 & 0 & 0 & 0 \end{pmatrix}. \tag{26}$$

The filtering is carried out for forced systems with the deterministic forcing in (1) given by

$$f(t) = A_f e^{i\omega_f t}, \tag{27}$$

where the amplitude is $A_f = 1$ and the frequency is $\omega_f = 0.15$. The number of assimilation cycles is chosen so that in each case the model is run for about 20 periods of the deterministic forcing. A number of tests of the filter performance for both correct and incorrect parameter values are discussed in Sections 7, 7.2.1, 8, 8.2.1,9.

5. Filtering with perfect model

The performance of a perfect filter, i.e., a filter which is not affected by model error, provides a benchmark for the subsequent analysis of skill of imperfect filters. As discussed in Section 4, we use the same system for generating the synthetic truth and for filtering the observed signal. Thus, the perfect filter here is given by SPEKF (cf. Section 3.2.1) which uses the nonlinear model (1) with exact formulas for the second-order statistics and correctly specified parameters, i.e., $\Lambda^M = \Lambda$ (see (25), (24)).

5.1. Measure of filter skill and parameter estimation

We measure how well a filter reproduces the truth signal (we refer to this property as skill) by means of the root mean square difference (RMS) between the true signal, $\{x_m\}_{m=1,\ldots,M}$, and the filtered solution, $\{\bar{x}_{m|m}\}_{m=1,\ldots,M}$, recorded at the same sequence of times of length M.

Please cite this article in press as: M. Branicki et al., Filtering skill for turbulent signals for a suite of nonlinear and linear extended Kalman filters, J. Comput. Phys. (2011), doi:10.1016/j.jcp.2011.10.029

We start by introducing some notions used for quantifying filter the performance:

Definition (*RMS error*). The RMS difference (or RMS error) between the truth sequence $\{x_m\}_{m=1,\dots,M}$ and the filtered solution $\{\bar{x}_{m|m}\}_{m=1,\dots,M}$ is defined as

$$RMS(x) = \sqrt{\frac{1}{M}\sum_{m=1}^{M} |\bar{x}_{m|m} - x_m|^2}. \tag{28}$$

The RMS error is computed independently for each component of the filtered signal after discarding the initial transient onto the attractor.

Definition (*Filter skill*). Consider filtering a turbulent signal at a single spatial location based on a sequence of observations $\{v_m\}_{m=1,\dots,M}$ at times $\{t_1,\dots,t_M\}$ and assume the truth $\{x_m\}_{m=1,\dots,M}$ at the same time sequence is known. We say that the filter has a *skill* for filtering the observed component $u(t)$ in (1) when the RMS error between the truth and the filtered solution is smaller than the observation error.

The accuracy of estimation of the unobserved components is judged by comparing the RMS errors between the estimated components and the synthetic truth.

Definition (*Filter divergence*). We define *filter divergence* as the outcome of the filtering procedure when the average RMS error in estimated signal exceeds the observation error.

Remark. Note that in our special case for a single Fourier mode $u(t)$ in (1) filter divergence means that simply trusting the observations provides a better estimate of the true signal than when running a divergent filter. When filtering a spatially extended turbulent system with sparse observations in the spatial domain the above definitions do not apply. Even if the RMS error of the filtered solution is large, there are not enough points on the physical grid for reconstructing the signal everywhere in the domain solely from the observations; thus, in such a case filters can have significant skill while exceeding (pointwise) the observation error [23,24,41].

5.2. Performance of the perfect filter in various dynamical regimes

The filtering skill of the perfect model and parameter estimation in each dynamical regime outlined in Section 2.1 depends also on the observation time Δt^{obs} and the observation noise variance r^o. We distinguish four general cases characterized by different performance of the perfect filter. Each case is associated with different ratio between the decorrelation times of the resolved variable $u(t)$ and the unresolved variable $\gamma(t)$. (The decorrelation time of $u(t)$ is given approximately by $1/\hat{\gamma}$, and the decorrelation time of $\gamma(t)$ is $1/d_\gamma$, as discussed in Section 2.1).

Case 1: $\boldsymbol{1}/\boldsymbol{d}_\gamma < \Delta \boldsymbol{t}^{\boldsymbol{obs}} \ll \boldsymbol{1}/\hat{\gamma}$ (Regimes I, II). *Observation time small compared to the decorrelation time of u(t) but longer than the decorrelation time of γ(t).*
- Good skill in filtering the observed signal $u(t)$.
- Mean values of $\gamma(t)$ and $b(t)$ recovered. Extrema of instability (i.e., dominant negative minima of $\gamma(t)$) detected.

Filtering with the perfect model has a high skill here. The observation time is too long to resolve the dynamics of $\gamma(t)$ but the mean values of both stochastic parameters are recovered correctly. Accurate estimation of γ is not essential for skillful filtering of u as long as the extrema of instability are detected (see Figs. 1 and 3). For small observation noise the filter trusts the observations and the improvement of the filtering skill due to a good model is negligible. For sufficiently large observation noise levels the filter trusts the model and fails to detect many unstable events but it still outperforms the observations (see Fig. 2).

Case 2: $\Delta \boldsymbol{t}^{\boldsymbol{obs}} < \boldsymbol{1}/\boldsymbol{d}_\gamma < \boldsymbol{1}/\hat{\gamma}$ or $\Delta \boldsymbol{t}^{\boldsymbol{obs}} < \boldsymbol{1}/\hat{\gamma} < \boldsymbol{1}/\boldsymbol{d}_\gamma$ (Regimes I-III). *Observation time step shorter than decorrelation times of both γ(t) and u(t).*
- Good skill in filtering the observed signal $u(t)$.
- $\gamma(t)$, including its dominant negative minima recovered well. $b(t)$ is estimated well if its decorrelation time is sufficiently long (i.e., $\Delta t^{obs} \ll 1/\gamma_b$).
  This is similar to Case 1, but here the signal is sampled sufficiently frequently so that the filter learns enough about $\gamma(t)$ to capture its most important features (see Figs. 8–10).

Case 3: $\boldsymbol{1}/\hat{\gamma} < \Delta \boldsymbol{t}^{\boldsymbol{obs}} \ll \boldsymbol{1}/\boldsymbol{d}_\gamma$ (Regimes II, III). *Observation time step small compared to the decorrelation time of γ(t)* but longer than that of $u(t)$.
- Only low frequency modulation recovered in $u(t)$.
- Mean value of $\gamma(t)$ and $b(t)$ recovered.
  In this case the observed signal decorrelates between the successive observations and filtering does not provide substantial improvement over the observations.

Please cite this article in press as: M. Branicki et al., Filtering skill for turbulent signals for a suite of nonlinear and linear extended Kalman filters, J. Comput. Phys. (2011), doi:10.1016/j.jcp.2011.10.029

Regime I. Filtering with perfect model.

The mean stability parameter: $\chi = -0.7$.
Observation time: $\Delta t^{obs} = 0.2$
Decorrelation time of u: $1/\hat{\gamma} \approx 0.833$
True signal parameters: $\hat{\gamma} = 1.2, d_\gamma = 20, \sigma_\gamma = 20, \quad \omega_u = 1.78, \sigma_u = 0.5, \quad \gamma_b = 0.5, \omega_b = 1, \sigma_b = 0.5.$
Observation error: $\sqrt{r^o} = 0.316$

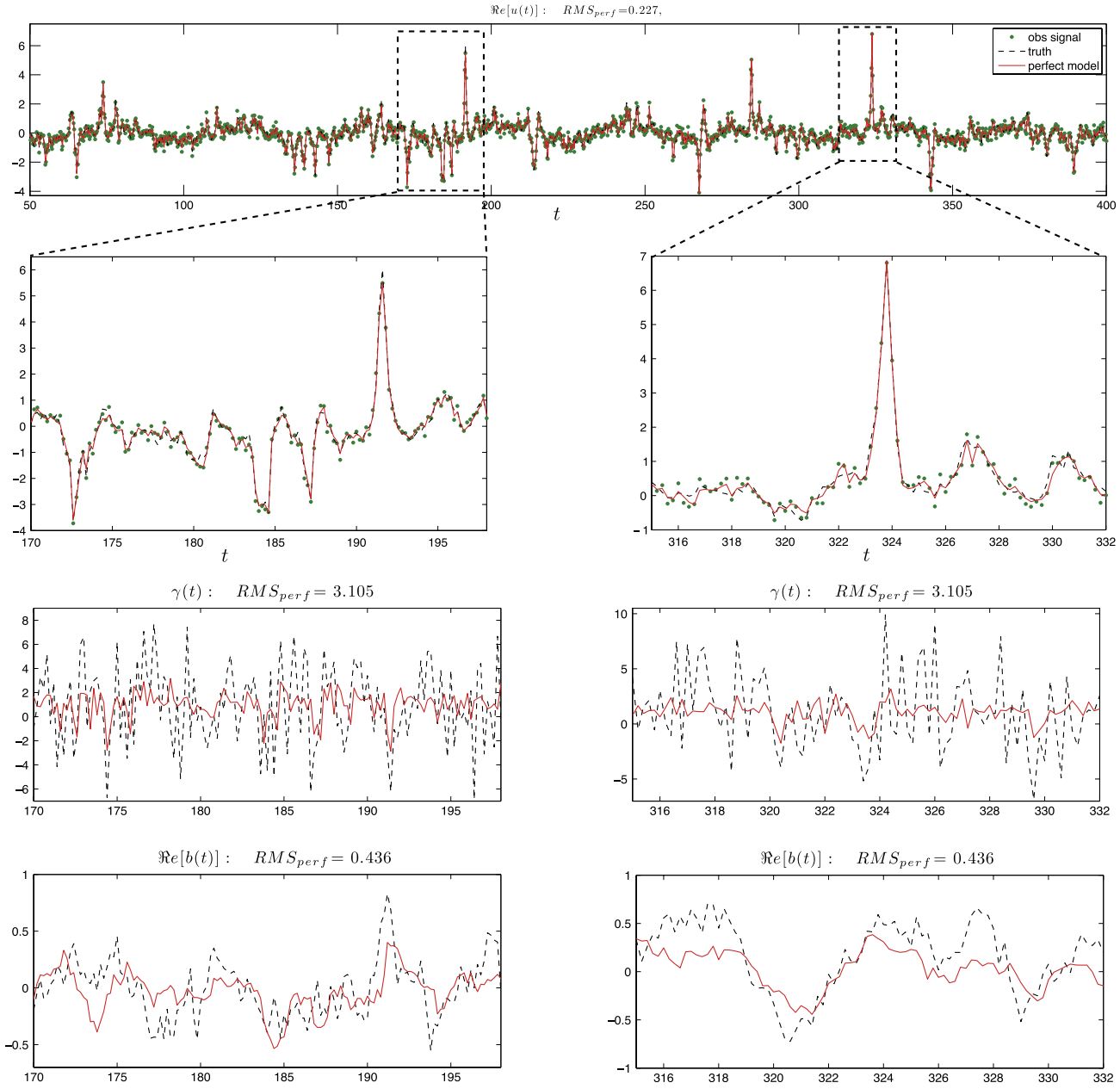

Fig. 1. (Regime I) Path-wise example of filtering with perfect model for small observation noise. The perfect filter is given here by SPEKF with correct system parameters (see Section 5).

Case 4: $\Delta t^{obs} \gg 1/\hat{\gamma} > 1/d_\gamma$ or $\Delta t^{obs} \gg 1/d_\gamma > 1/\hat{\gamma}$ (Regimes I-III). *Observation time step long compared to decorrelation times of both $\gamma(t)$ and $u(t)$.*

- Only low frequency modulation due to periodic forcing is recovered in $u(t)$.
- The estimation of $\gamma(t)$ and $b(t)$ is completely unreliable.

In this case the observed signal decorrelates between the subsequent observations and the filter dampens whatever information is acquired from the observations by the next analysis time. Consequently, only the low-frequency modulation due to the deterministic forcing is recovered in the filtered solution. The flow of information from the observations of $u(t)$ to the dynamics of γ and b is weak and the parameter estimation is poor.

Please cite this article in press as: M. Branicki et al., Filtering skill for turbulent signals for a suite of nonlinear and linear extended Kalman filters, J. Comput. Phys. (2011), doi:10.1016/j.jcp.2011.10.029

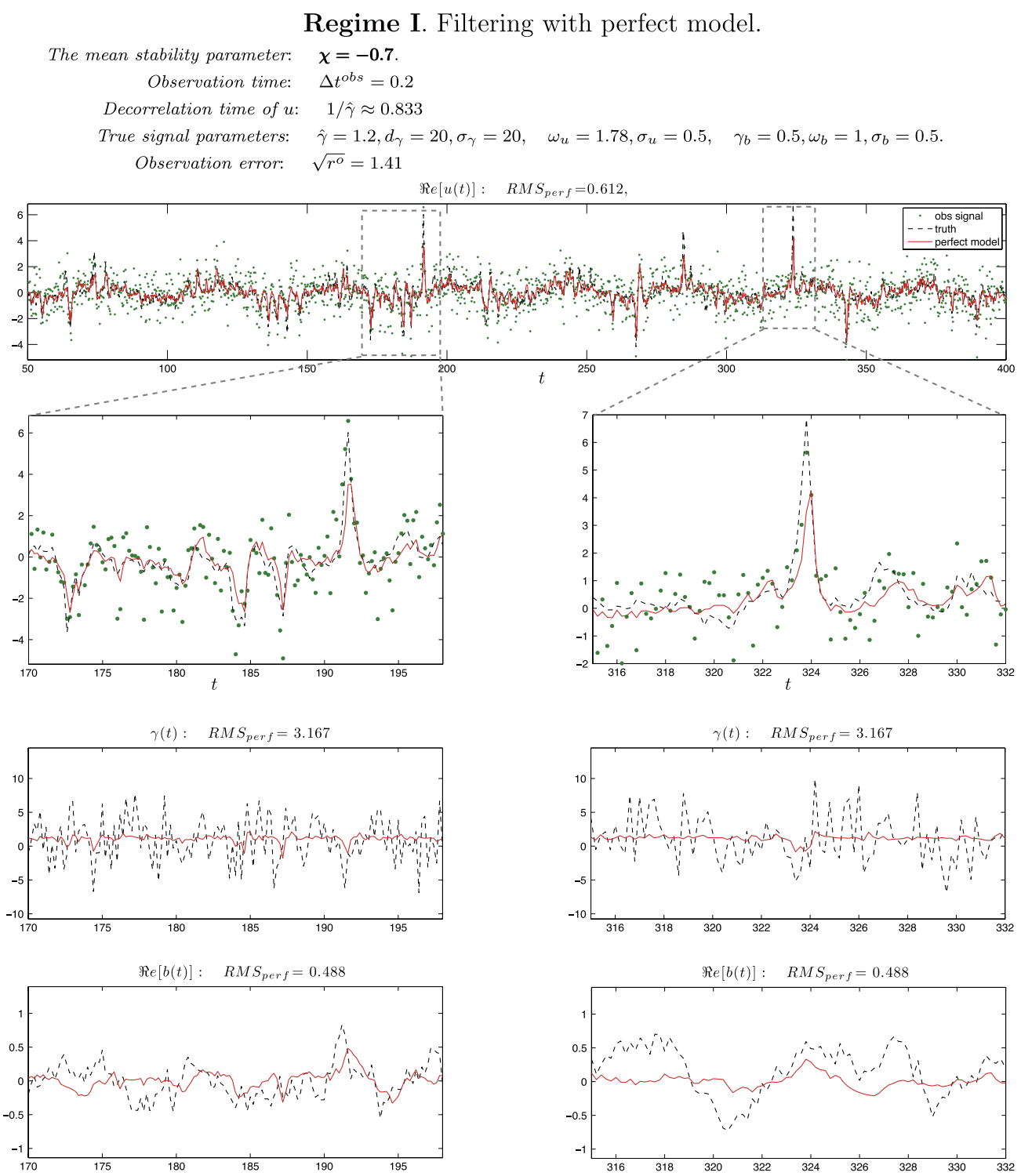

Fig. 2. (Regime I) Path-wise example of filtering with perfect model when the signal is dominated by noise but the observation time is much shorter than the decorrelation time of $u(t)$. The perfect filter is given here by SPEKF with correct system parameters (see Section 5).

6. Filtering with model error

An unambiguous assessment of the effects of model error on the filtering skill is often difficult since its properties are unknown almost by definition. In the case of Bayesian filters using stochastic parameter estimation, such as the filters discussed here, the sources of model error in imperfect filters arise from:

- *Imperfect forecast models used for filtering.* These model errors affect, in principle, all of the filters discussed here (i.e., SPEKF, GCF, DMF, SDMF, TEKF; see Section 3).

Please cite this article in press as: M. Branicki et al., Filtering skill for turbulent signals for a suite of nonlinear and linear extended Kalman filters, J. Comput. Phys. (2011), doi:10.1016/j.jcp.2011.10.029

- *Incorrect statistics* used in the filters due to particular moment closure approximations. In our setting, these errors affect GCF, DMF, SDMF and TEKF.

The two sources of model error listed above are, in general, interdependent. However, the use of system (1) with exactly solvable statistics for generating the synthetic truth and as the forecast model in all filters allows for the following two classes of tests to be carried out:

- *Filtering with correctly specified parameters (i.e. $\Lambda^M = \Lambda$; see Section 4).* In this case the effects of model error arising solely due to incorrect statistics in the filtered solutions can be examined.
- *Filtering with incorrectly specified filter parameters (i.e. $\Lambda^M \neq \Lambda$).* This configuration can be used to study the robustness and importance of the effects of incorrect statistics on the skill of the imperfect filters in the presence of additional model error due to an imperfect knowledge of the model parameters under the hypothesis of perfect model structure (see, for example, [37] in a different context).

A remark is in order here concerning our consideration of error in the imperfect forecast models only due to the imprecision in parameter values. The use of incorrect model parameters in our filtering procedure corresponds to introducing multiplicative and additive biases into the forecast model and one can consider such a setup as a case of structurally perfect model where inadequate parameterization of unresolved physical processes is represented only by these two types of 'bulk' error terms. Of course, if a posteriori analysis and predictive checks of the forecast model can be carried out, the model covariance can be inflated to minimize the so-called *innovation variance* (see, e.g., [34]) in order to reduce the model error; alternatively, an improved bias model can be employed in the augmented forecast model [5]. However, as already pointed out earlier, we focus here on filtering techniques which are capable of real-time state and parameter estimation for subsequent predictions, i.e. the underlying assumption is that limited or no posterior (off-line) analysis can be carried out and one requires a rapidly deployable model which is computationally cheap, flexible, robust and as skillful as possible. While the assumption of the perfect model structure is certainly limited, it allows here for an additional validation of the effects of errors due to incorrect statistics beyond the perfect model scenario; we also point out that even the use of estimated parameters alone from filtering in the initial data for prediction has been shown to enhance the prediction skill [22]. Moreover, additive and multiplicative biases in model parameters are commonly used by ECMWF Ensemble Prediction System as an operational representation of model error [9,51]. The real-time incorporation of innovations from data assimilation is a future research topic planned by the authors.

The procedure outlined above for analyzing the filter skill is carried out next in the three regimes mimicking different modes in the turbulent spectrum and discussed in Section 2.1. This comprehensive study also provides insight into the robustness of different filters in a wide range of physical conditions; filter robustness is a critical feature when dealing with high-dimensional, spatially-extended turbulent systems.

7. Filter performance and parameter estimation in regime with plentiful short-lasting, transient instabilities (Regime I)

In this and the subsequent two sections we study the skill of the filters derived in Section 3 for reconstructing the observed signal $u(t)$ and estimating the hidden stochastic parameters $\gamma(t)$ and $b(t)$. All tests are carried out for signals generated in different regimes of mean-stable dynamics of (1) which were discussed in Section 2.1. Description of detailed tests of filtering skill for varying observation time step, observation noise variance, and incorrect filter parameters is preceded by a summary of the most important findings.

7.1. Characteristics of the filtered signal

The configuration considered here corresponds to regime I (cf. Section 2.1) of the mean-stable dynamics of the system (1) and it is characterized by very frequent but short and intermittent phases of transient instability in the dynamics of $u(t)$. The ability of the filters to detect these intermittent instabilities largely determines the filter skill. The decorrelation time of fluctuations in $\gamma(t)$, given by $1/d_\gamma$, is very small here. The decorrelation time of fluctuations in $u(t)$, given approximately by $1/\hat{\gamma}$, is controlled by the mean damping $\hat{\gamma}$ which can vary widely since the mean-stability condition (2) does not impose an upper bound on $\hat{\gamma}$ in this regime. Both the the mean damping strength of $u(t)$ and the separation between decorrelation times of $u(t)$ and $\gamma(t)$ have important consequences on the filtering skill.

We distinguish the following three subcategories of dynamical behavior in this regime:

- *Strongly damped dynamics* of $u(t)$ with small-amplitude fluctuations around low-frequency deterministic mean: In this case $\hat{\gamma} \gg 1$, the mean-stability parameter $\chi \ll -1$, and the decorellation times of fluctuations in both $\gamma(t)$ and of $u(t)$ are very short.
- *Weakly damped dynamics of $u(t)$* with very large fluctuations: In this case $\hat{\gamma}$ is small and $0 < \chi \ll 1$ so that the system is marginally mean-stable. The decorrelation time of fluctuations in $u(t)$ is long compared to the decorrelation time of $\gamma(t)$.

Please cite this article in press as: M. Branicki et al., Filtering skill for turbulent signals for a suite of nonlinear and linear extended Kalman filters, J. Comput. Phys. (2011), doi:10.1016/j.jcp.2011.10.029

- *Moderately damped dynamics of u(t)* with large-amplitude, intermittent fluctuations: Here $\hat{\gamma} \sim \mathcal{O}(1)$ and the mean-stability parameter, $-\chi \sim \mathcal{O}(1)$. The decorrelation time of fluctuations in $u(t)$ is well separated from the very short decorrelation time of fluctuations in $\gamma(t)$.

In the numerical tests we have chosen the truth signals generated from (1) with moderately damped dynamics so that the low-frequency modulation is significantly affected, but not completely dominated, by the transient instabilities. The truth signal in the simulations was generated with

$$\hat{\gamma} = 1.2, d_\gamma = 20, \sigma_\gamma = 20, \quad \omega_u = 1.78, \sigma_u = 0.5, \gamma_b = 0.5, \omega_b = 1, \sigma_b = 0.5; \tag{29}$$

(see Fig. 1 for an example of a path-wise solution). For parameters (29) the mean stability parameter is $\chi = -0.7$ and the decorrelation times of u and γ are well separated and given respectively by $1/\hat{\gamma} \approx 0.833$ and $1/d_\gamma = 0.05$. The interplay between the low-frequency modulation and the intermittent instabilities provides a good test bed for analyzing the effects of various sources of model error on the filtering skill.

7.2. Filtering with imperfect models

We first summarize the most important characteristics of filtering with model error due to incorrect statistics in regime I. Skill of the perfect filter in this regime was discussed in Section 5 (see Cases 1, 2, 4). Description of specific tests carried out, as well as the figures illustrating the dependence of filter skill on the observation time, observation noise variance and incorrect parameter values, are presented in Section 7.2.1.

Filter performance in regime I:

- For filter parameters $\left\{d_\gamma^M \geqslant d_\gamma, \sigma_\gamma^M \leqslant \sigma_\gamma, \sigma_u^M \leqslant \sigma_u\right\}$, i.e., underestimated decorrelation time and noise in the hidden damping fluctuations $\gamma(t)$, and underestimated noise in the observed variable $u(t)$, the skill hierarchy of the analyzed filters is
  $SPEKF \gtrsim GCF \gtrsim DMF > SDMF > TEKF$

  For small observation time steps ($\Delta t^{obs} \ll 1/\hat{\gamma}$) the skill of all filters is good and comparable. The skill differences increase monotonically with Δt^{obs} and r^o but the the above hierarchy remains unchanged. In other regimes of incorrect filter parameters the skill of SPEKF is somewhat worse than that of GCF and DMF and in extreme cases it may become comparable with TEKF (Figs. 7 and 5); however, in such cases all filters tend to have a good skill. For noise dominated signals all filters have comparable skill and moment closure errors are negligible.
- Effects of model error due to the moment closure approximations in the imperfect filters are most pronounced in this regime (compare Figs. 7 and 14). For correct model parameters the errors due to neglecting the second moments in the model mean (16a) are comparable to those arising from neglecting the third moments in the model covariance (16b) (Fig. 7). These errors increase with the observation time step Δt^{obs} (Fig. 5).
- TEKF and SDMF diverge for large observation times, $\Delta t^{obs} \sim 1/\hat{\gamma}$, and small observation noise levels (Fig. 5); they are also sensitive to errors in the filter parameters - in particular, when $\Delta t^{obs} \sim 1/\hat{\gamma}$ and $d_\gamma^M \ll d_\gamma$ (overestimated decorrelation time of $\gamma(t)$), or when filtering with underestimated noise variances $\sigma_u^M, \sigma_\gamma^M$ (Fig. 7). These filters fail to resolve the large-amplitude bursts of instability in $u(t)$ (Figs. 3 and 4), except for very small Δt^{obs}. The skill of these filters becomes comparable to the skill of the other filters for strongly damped dynamics of $u(t)$ (i.e., $\hat{\gamma} \gg 1$ and few large-amplitude transient instabilities; not shown).
- SPEKF in regime I is the best filter for underestimated decorrelation time of $\gamma(t)$ (i.e., $d_\gamma^M \gg d_\gamma$), indicating significant moment closure errors in the other filters (Fig. 7). SPEKF is the best at capturing the dominant negative minima of $\gamma(t)$ which improves its skill (see, e.g., Fig. 3). Its performance deteriorates for significantly overestimated decorrelation time of damping fluctuations (i.e., $d_\gamma^M \ll d_\gamma$).
- GCF is the least sensitive filter to parameter errors in regime I but it has lower skill than SPEKF for $\left\{d_\gamma^M \geqslant d_\gamma, \sigma_\gamma^M \leqslant \sigma_\gamma, \sigma_u^M \leqslant \sigma_u\right\}$ (Fig. 7). The errors due to the Gaussian closure are small and only become noticeable (compared to the perfect filter) at large observation times ($\Delta t^{obs} \sim 1/\hat{\gamma}$) and noise variances r^o (Figs. 5, 7). The robustness of GCF stems largely from its tendency to underestimates covariances when compared to SPEKF; for incorrect parameters SPEKF propagates the incorrect statistics more accurately which can lead to more spurious results (especially for $d_\gamma^M \ll d_\gamma$; Fig. 7).
- DMF has a similar skill to GCF for small observation times. For $\Delta t^{obs} \sim 1/\hat{\gamma}$, the errors due to neglecting the second moments in the mean used by DMF deteriorate its skill for underestimated decorrelation times of γ (i.e., $d_\gamma^M > d_\gamma$); however, this make it less susceptible to overestimated decorrelation times of γ (Fig. 7).

Parameter estimation in regime I:

- As expected, the estimation of the hidden dynamics of the stochastic parameters in this regime is generally poor but the means of $\gamma(t)$ and $b(t)$ are recovered well by SPEKF, GCF and DMF (Figs. 1–4).

Please cite this article in press as: M. Branicki et al., Filtering skill for turbulent signals for a suite of nonlinear and linear extended Kalman filters, J. Comput. Phys. (2011), doi:10.1016/j.jcp.2011.10.029

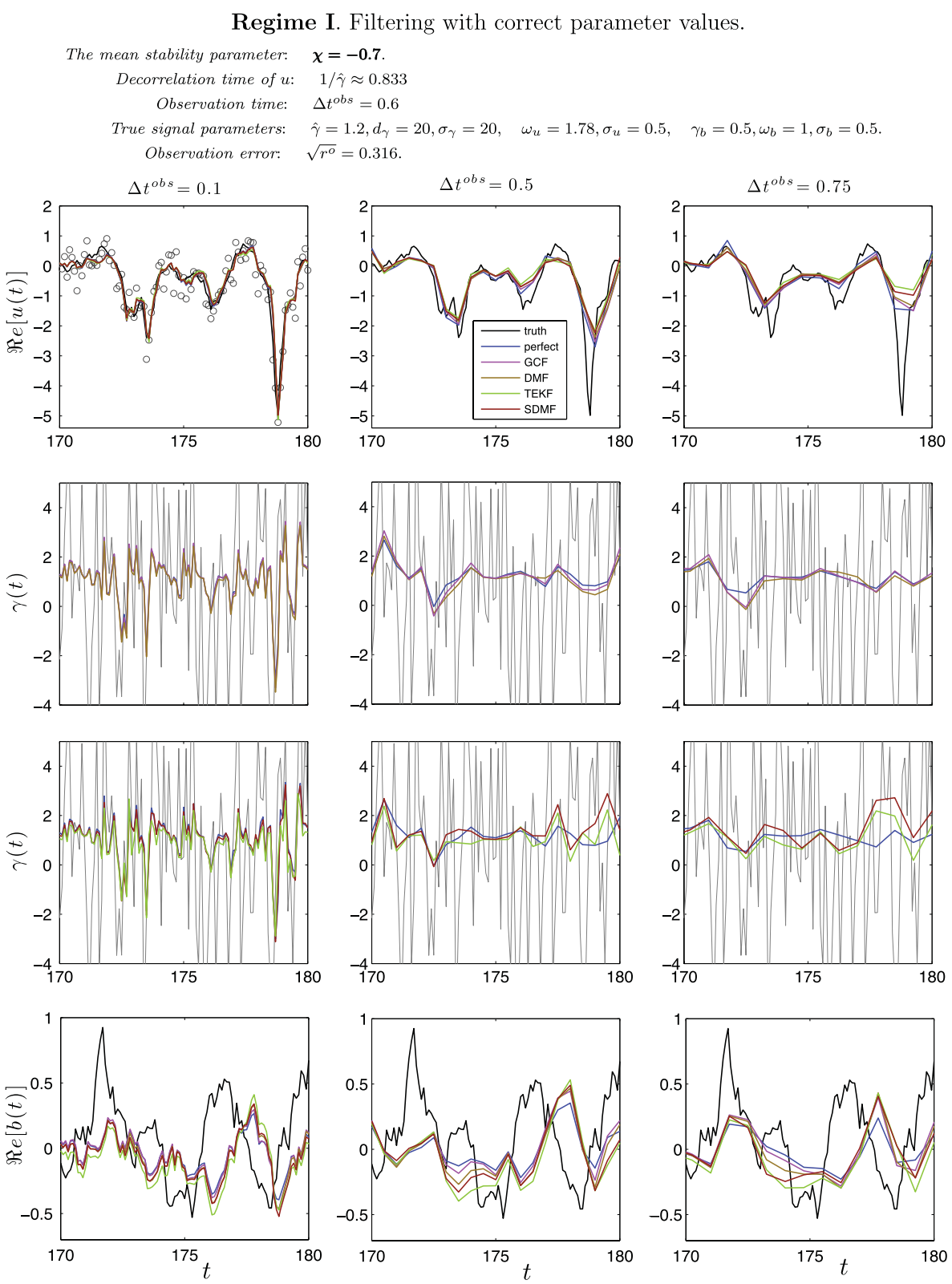

Fig. 3. (Regime I) Path-wise example of filtering with correct system parameters for three different values of the observation time Δt^{obs}. The suite of filters used here is described in Section 3.

- SPEKF, GCF and DMF have a similar skill for estimating $\gamma(t)$. For small and moderate observation times (i.e. $\Delta t^{obs} < 1/\hat{\gamma}$) these filters also detect the dominant negative minima of $\gamma(t)$ from the observations of $u(t)$ (Fig. 4) which greatly improves their filtering skill. The estimation of $\gamma(t)$ in other regions is unreliable.

Please cite this article in press as: M. Branicki et al., Filtering skill for turbulent signals for a suite of nonlinear and linear extended Kalman filters, J. Comput. Phys. (2011), doi:10.1016/j.jcp.2011.10.029

Regime I. Filtering with incorrect parameter values.

The mean stability parameter: $\chi = -0.7$.
Decorrelation time of u: $1/\hat{\gamma} \approx 0.833$
Observation time: $\Delta t^{obs} = 0.6$
True signal parameters: $\hat{\gamma} = 1.2, d_\gamma = 20, \sigma_\gamma = 20, \quad \omega_u = 1.78, \sigma_u = 0.5, \quad \gamma_b = 0.5, \omega_b = 1, \sigma_b = 0.5.$
Observation error: $\sqrt{r^o} = 0.316.$

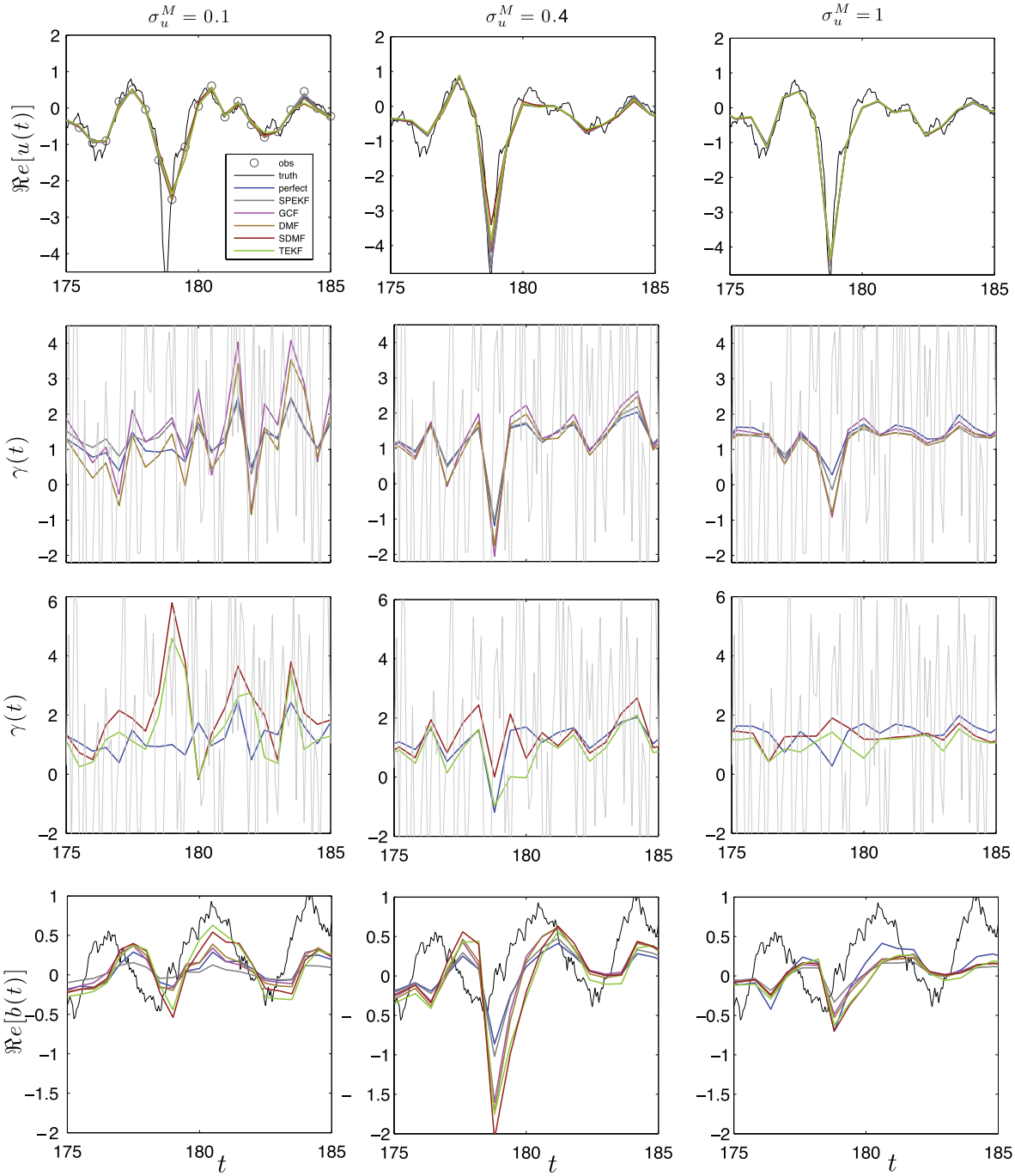

Fig. 4. (Regime I) Example of path-wise filtering with incorrect parameter values for three different values of the noise amplitude σ_u^M assumed in the filters for the dynamics of $u(t)$. The suite of filters used here is described in Section 3.

- The estimation of $\gamma(t)$ by TEKF and SDMF is similar to the other filters when filtering with correct parameters and small observation times (Fig. 3). For incorrect filter parameters, these filters are completely unreliable at estimating $\gamma(t)$ (see Fig. 4).

Please cite this article in press as: M. Branicki et al., Filtering skill for turbulent signals for a suite of nonlinear and linear extended Kalman filters, J. Comput. Phys. (2011), doi:10.1016/j.jcp.2011.10.029

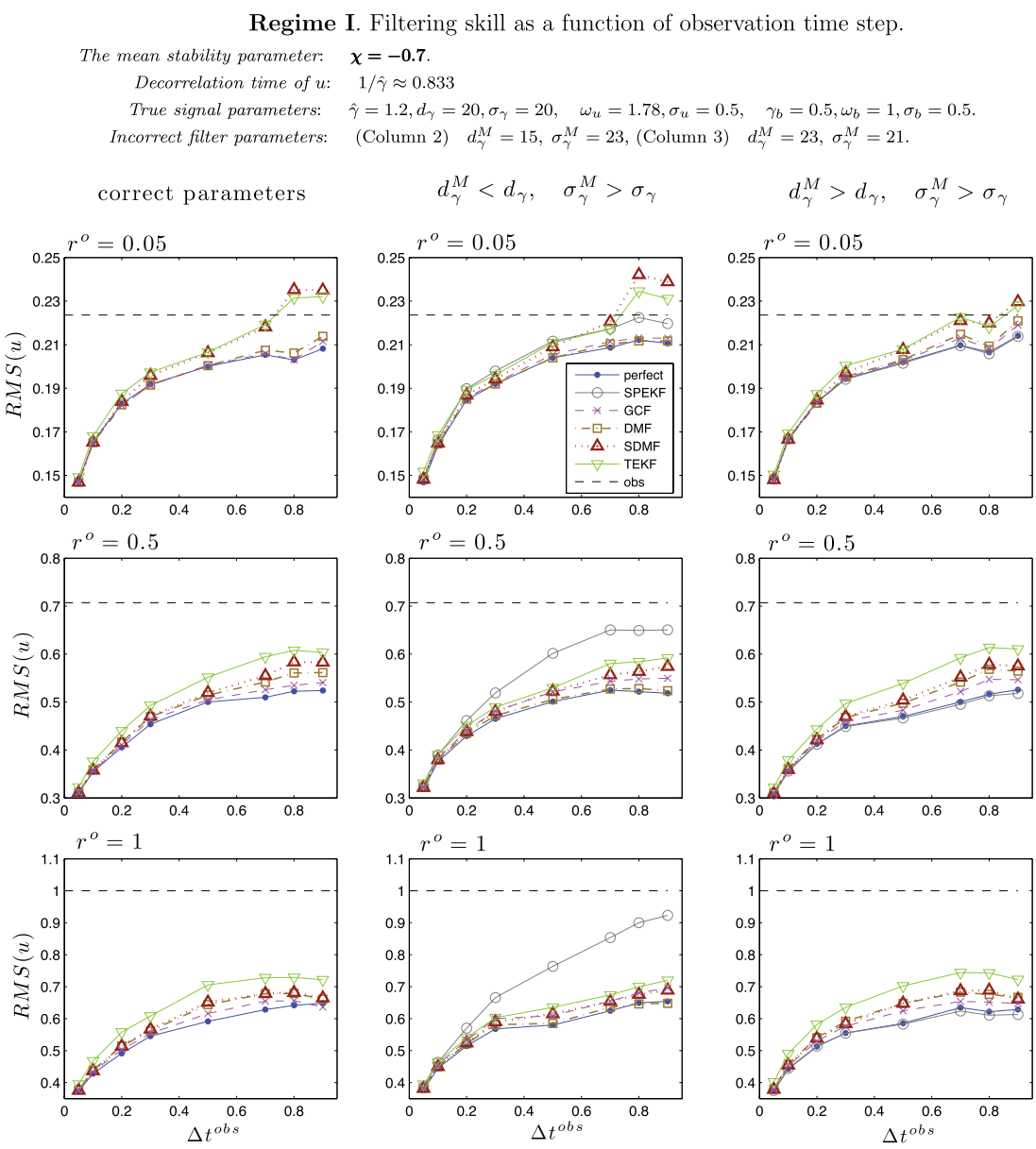

Fig. 5. (Regime I) Average RMS errors of the filtered solution $u(t)$ as a function of the observation time Δt^{obs} for fixed values of the observation noise variance r^o and different filter parameters. For $r^o \gtrsim 1$ the signal is dominated by noise. The filters used here are described in Section 3.

- For sufficiently short observation times, i.e., when $\Delta t^{obs} < 1/\gamma_b$, all filters estimate the additive bias, $b(t)$, similarly well with a characteristic lag between the minima in the filtered signal and true $b(t)$ (Figs. 3,4).

7.2.1. Specific examples

We discuss here the results of specific tests of filter skill in our suite of filters in regime I as a function of the observation time step, observation noise variance, and incorrect filter parameters.

Path-wise examples of filtering in regime I (Figs. 1,2,3,4)

In Figs. 1 and 2 we show two examples of filtering with the perfect filter which, as discussed earlier, is given by SPEKF with correct parameter values. In both examples the observation time step is much shorter than the decorrelation time of $u(t)$. Fig. 1 shows results of filtering and stochastic parameter estimation for the observation noise variance $r^o = 0.1$ which, for the system parameters (29), corresponds to a moderate signal-to-noise ratio. The observation time here is too long to resolve the dynamics of $\gamma(t)$ but its mean value is recovered correctly. Accurate estimation of $\gamma(t)$ is not essential for skillful filtering of the resolved variable $u(t)$ as long as the dominant negative minima of the damping fluctuations are recovered. In Fig. 2 the observed signal is dominated by noise and the filter trusts the model, failing to detect many unstable events; however, it still outperforms the observations. The estimation of $\gamma(t)$ is unsurprisingly poor but some extrema of instability are still detected.

Figs. 3 and 4 show path-wise examples of filtering with the imperfect filters. Fig. 3 shows examples of filtering with correct parameters for three different observation times. Fig. 4 shows three examples of filtering with incorrect noise amplitude,

Please cite this article in press as: M. Branicki et al., Filtering skill for turbulent signals for a suite of nonlinear and linear extended Kalman filters, J. Comput. Phys. (2011), doi:10.1016/j.jcp.2011.10.029

Regime I. Filtering skill as a function of observation noise variance.

The mean stability parameter: $\chi = -0.7$.

Decorrelation time of u: $1/\hat{\gamma} \approx 0.833$

True signal parameters: $\hat{\gamma} = 1.2, d_\gamma = 20, \sigma_\gamma = 20, \quad \omega_u = 1.78, \sigma_u = 0.5, \quad \gamma_b = 0.5, \omega_b = 1, \sigma_b = 0.5.$

Incorrect filter parameters: (Column 2) $d_\gamma^M = 15,\ \sigma_\gamma^M = 23$, (Column 3) $d_\gamma^M = 23,\ \sigma_\gamma^M = 21.$

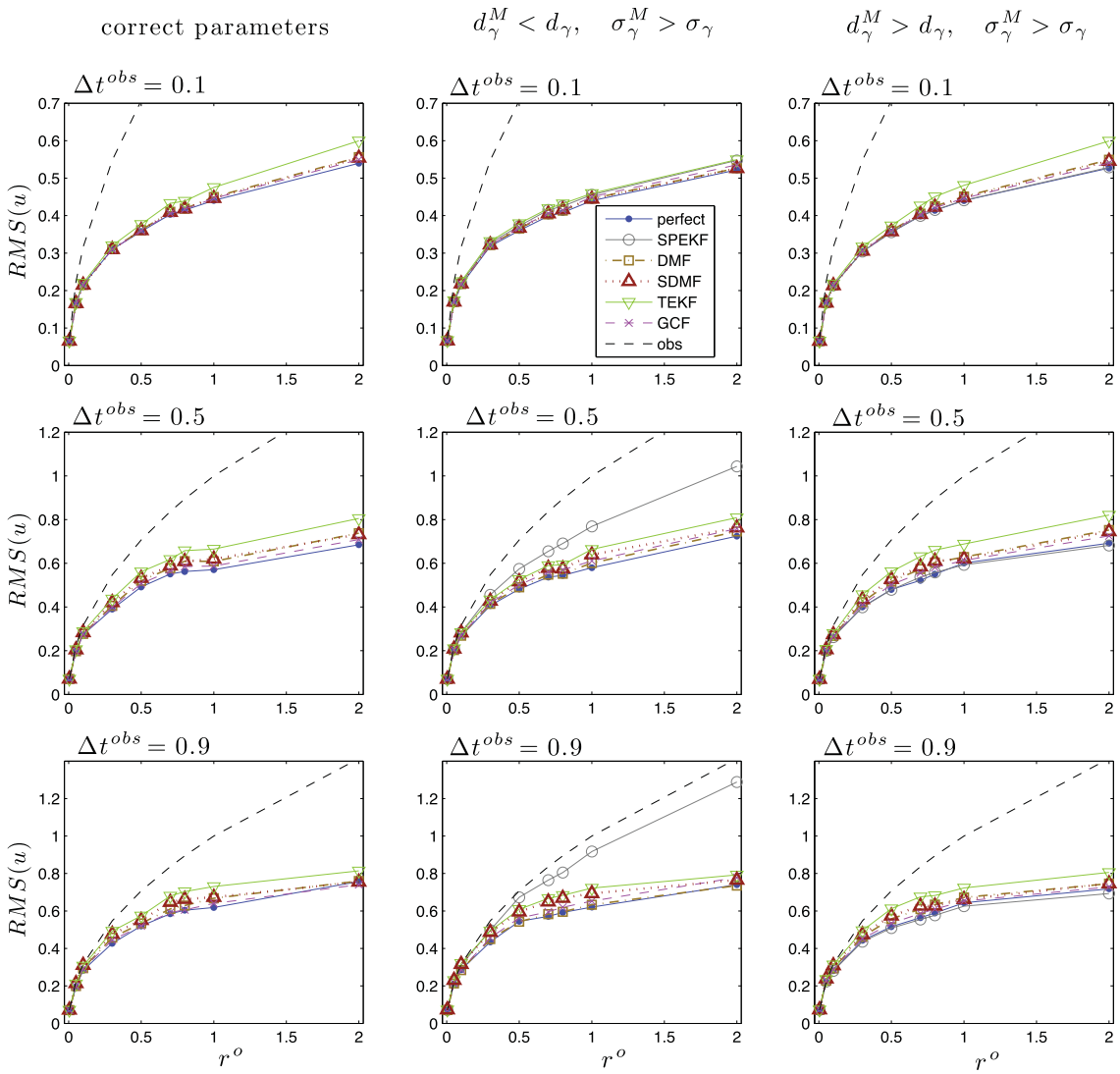

Fig. 6. (Regime I) Average RMS errors of the filtered solution $u(t)$ as a function of the observation noise variance r^o for fixed values of the observation time step Δt^{obs} and different filter parameters. For $r^o \gtrsim 1$ the signal is dominated by noise. The filters used here are described in Section 3.

σ_u^M, used by the filters in the dynamics of $u^M(t)$ and a relatively large observation time ($\Delta\ t^{obs} = 0.6$, decorrelation time $1/\hat{\gamma} = 0.83$). As in the perfect filter scenario, detection of the negative minima of $\gamma(t)$ is essential for skillful filtering of the resolved variable, $u(t)$. SPEKF, GCF and DMF clearly outperform TEKF and SDMF here. When filtering with large observation time steps (Fig. 3) many short-lasting unstable bursts in the truth signal are underresolved in the observations. These resolution deficiencies affect the performance of all filters even for correct parameters but SPEKF, GCF and DMF remain more skillful than SDMF and TEKF. When filtering with incorrect noise amplitudes σ_u^M, SPEKF has the best skill for recovering the extrema of instability, especially for $\sigma_u^M < \sigma_u$, but it is somewhat worse than GCF and DMF in other intervals.

Filtering skill in regime I as a function of observation time step (Fig. 5)

In Fig. 5 we show the average RMS errors of filtered solutions $u(t)$ which are obtained by sampling the same truth signal with different observation time steps, Δt^{obs}, for fixed values of the observation noise variance r^o. The particular values of r^o we have chosen are such that the smallest considered value, $r^o = 0.05$, corresponds to high overall signal-to-noise ratio, while for the largest considered value, $r^o = 1$, the signal is dominated by noise. The first column in Fig. 5 shows the RMS errors for filtering with correct parameters; in this case SPEKF is the perfect filter and GCF, DMF, SDMF, and TEKF, are affected only by model errors due to incorrect statistics (see Section 6). Columns 2 and 3 in Fig. 5 show the RMS errors of the estimated solution $u(t)$ when filtering with incorrect parameters. In column 2 of Fig. 5 all filters (except for the perfect filter) overestimate

Please cite this article in press as: M. Branicki et al., Filtering skill for turbulent signals for a suite of nonlinear and linear extended Kalman filters, J. Comput. Phys. (2011), doi:10.1016/j.jcp.2011.10.029

Regime I. Filtering with incorrect parameter values.

The mean stability parameter: $\chi = -0.7$.
Decorrelation time of u: $1/\hat{\gamma} \approx 0.833$
True signal parameters: $\hat{\gamma} = 1.2, d_\gamma = 20, \sigma_\gamma = 20, \quad \omega_u = 1.78, \sigma_u = 0.5, \quad \gamma_b = 0.5, \omega_b = 1, \sigma_b = 0.5.$
Incorrect filter parameters: σ_γ^M, d_γ^M, σ_u^M varied.

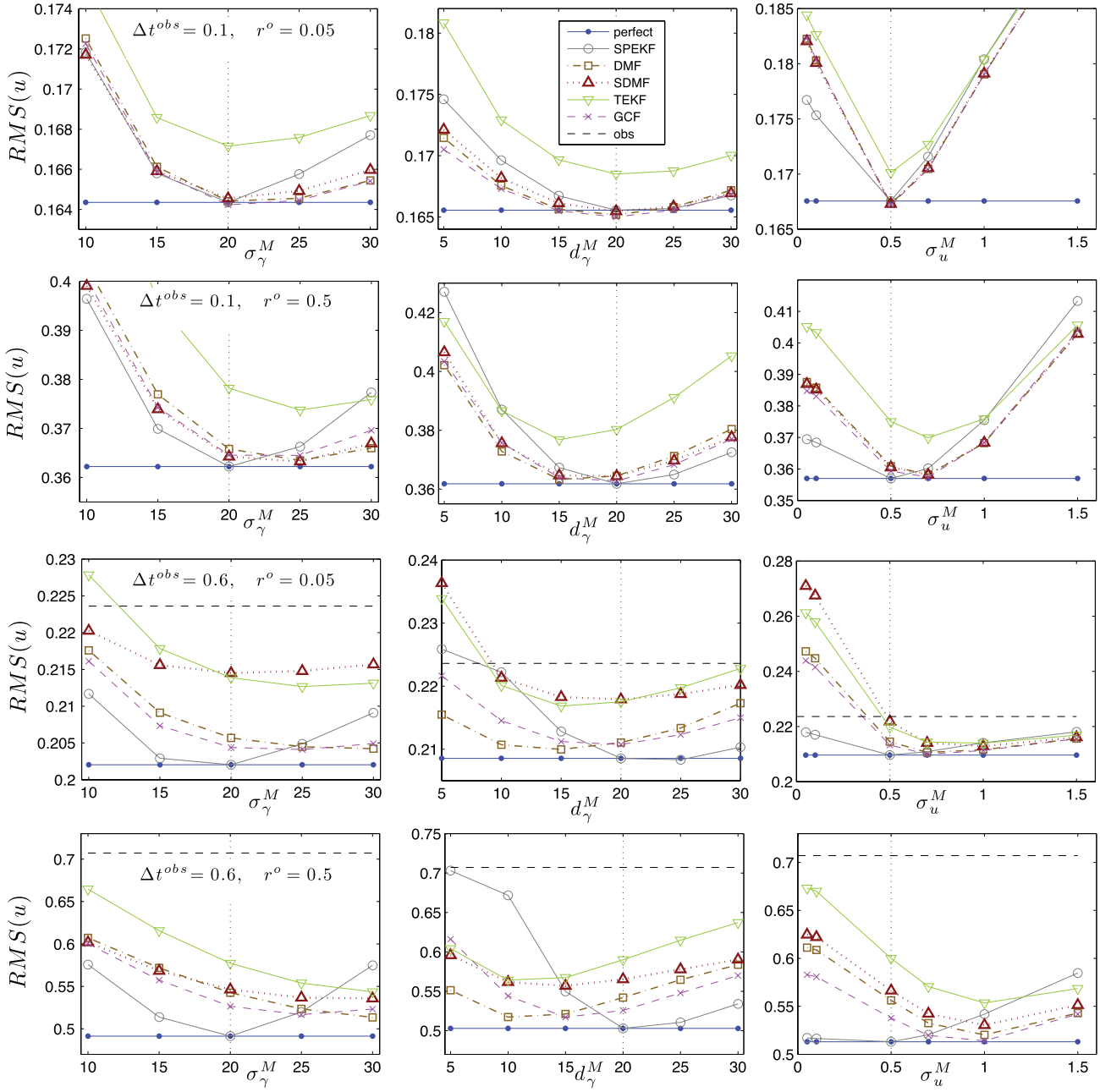

Fig. 7. (Regime I) Filtering with imperfect models (see Section 6). Average RMS errors of the filtered solution $u(t)$ as a function of the filter parameter σ_γ^M (i.e., incorrect noise amplitude assumed in γ) for fixed values of observation time Δt^{obs} and fixed observation noise variance r^o. The filter suite is described in Section 3.

the decorrelation time of the hidden damping fluctuations $\gamma(t)$ (i.e., $d_\gamma^M < d_\gamma$); in column 3 of Fig. 5 all filters underestimate the decorrelation time of $\gamma(t)$ ($d_\gamma^M < d_\gamma$).

Filtering skill in regime I as a function of observation noise variance (Fig. 6)

The dependence of filter skill on the observation noise levels is summarized in Fig. 6 which shows the average RMS errors of the filtered signal $u(t)$ as a function of the observation noise variance, r^o, for fixed values of the observation time step Δt^{obs} and for various combinations of filter parameters. The same truth signal as in the previous tests (see Fig. 1) was used here.

Please cite this article in press as: M. Branicki et al., Filtering skill for turbulent signals for a suite of nonlinear and linear extended Kalman filters, J. Comput. Phys. (2011), doi:10.1016/j.jcp.2011.10.029

Regime II. Filtering with correct parameters within distinct intervals.

The mean stability parameter: $\boldsymbol{\chi = -0.05}$.
Decorrelation time of u: $1/\hat{\gamma} \approx 1.81$
Observation time: $\Delta t^{obs} = 0.2$
True signal parameters: $\hat{\gamma} = 0.55, d_\gamma = 0.5, \sigma_\gamma = 0.5, \quad \omega_u = 1.78, \sigma_u = 0.1, \quad \gamma_b = 0.4, \omega_b = 1, \sigma_b = 0.4.$
Observation error: $\sqrt{r^o} = 0.316.$

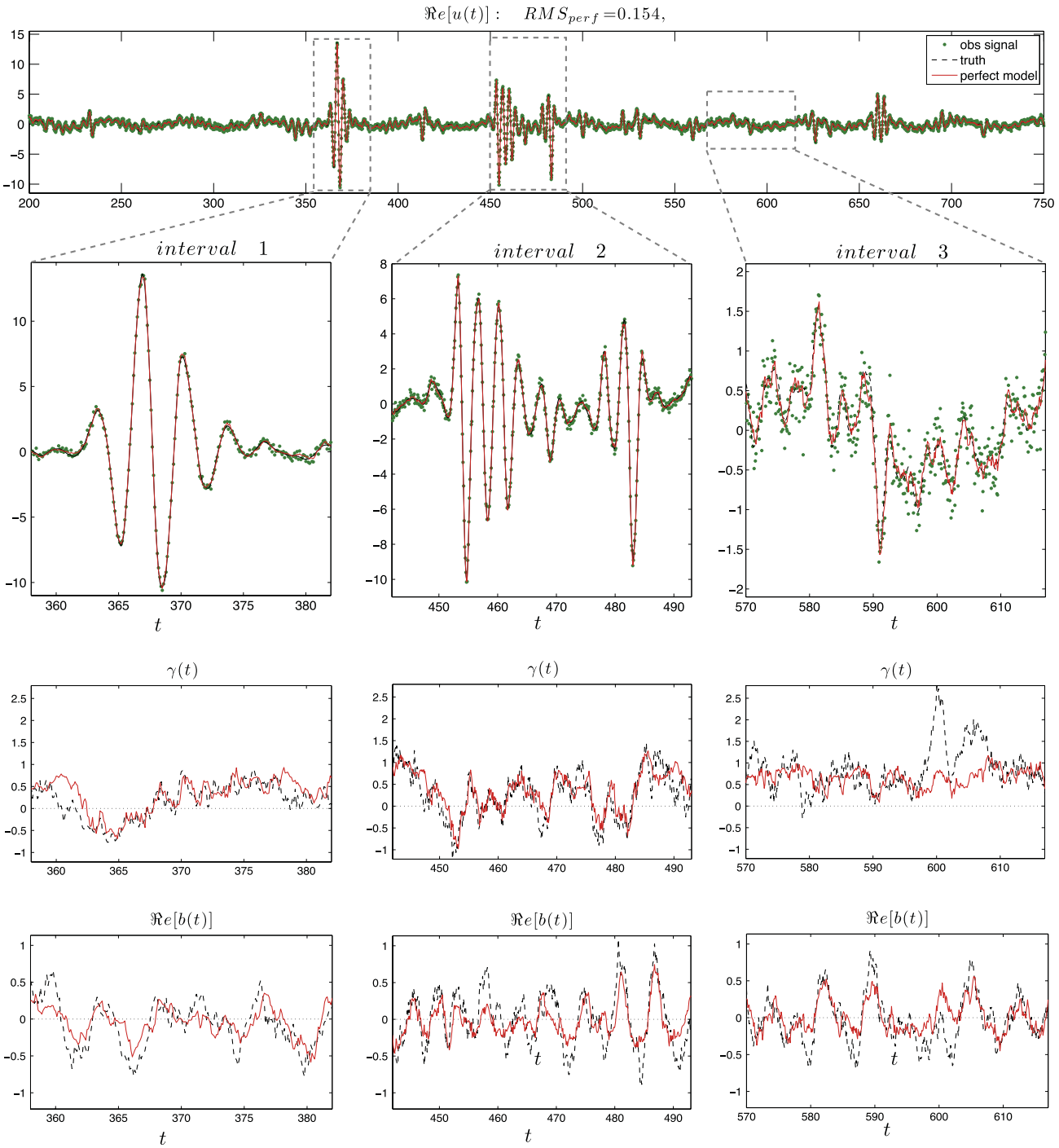

Fig. 8. (Regime II) Filtering with the perfect model within three dynamically distinct intervals: ***Interval 1***: large-amplitude transient instability in $u(t)$; ***Interval 2***: two subsequent instabilities dominating the low-frequency modulation; ***Interval 3***: quiescent phase with one short unstable episode. The perfect filter is given here by SPEKF with correct parameters (see Section 5).

Please cite this article in press as: M. Branicki et al., Filtering skill for turbulent signals for a suite of nonlinear and linear extended Kalman filters, J. Comput. Phys. (2011), doi:10.1016/j.jcp.2011.10.029

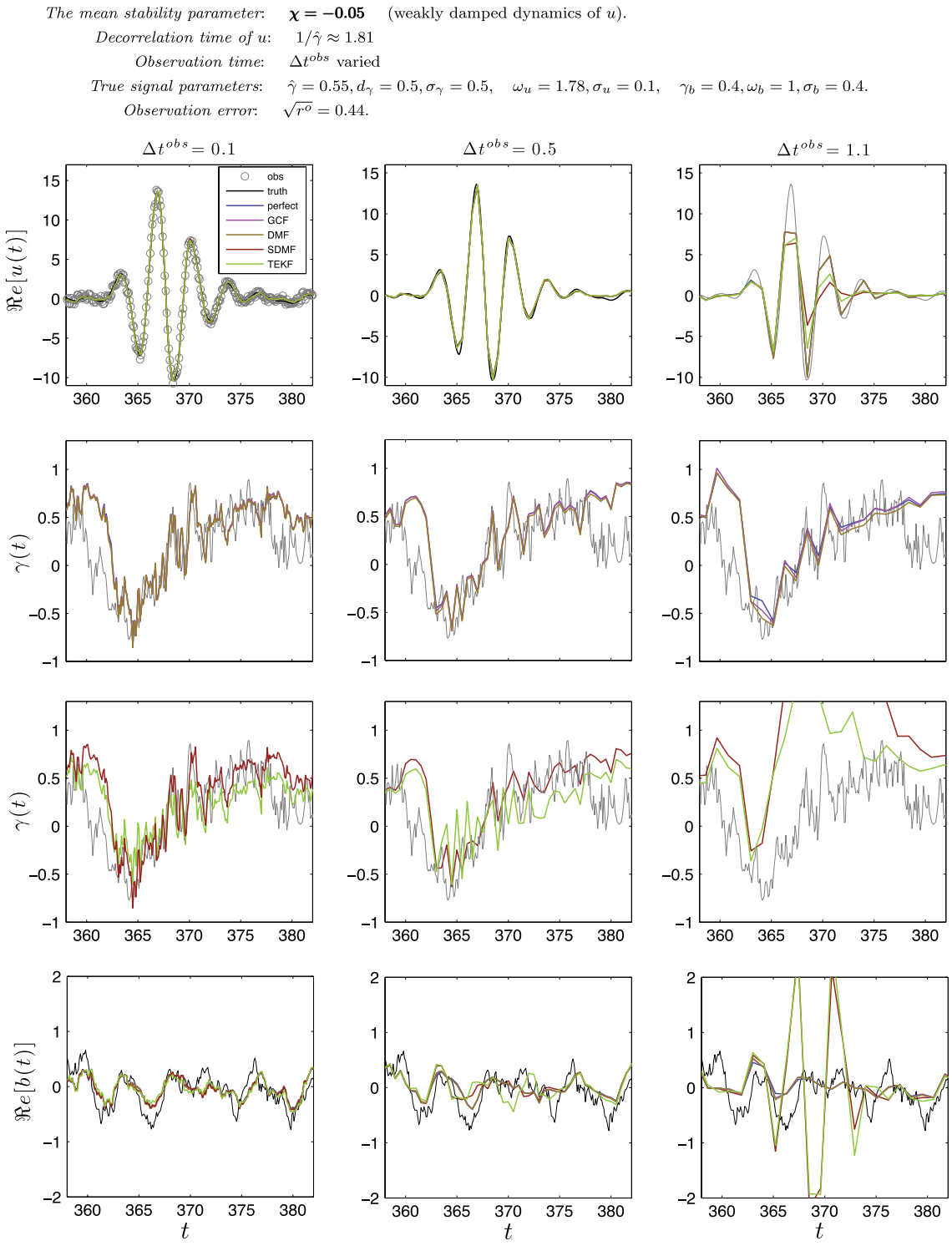

Fig. 9. (Regime II). Path-wise example of filtering within interval 1 (see Fig. 8) for three different observation times, Δt^{obs}, and a fixed value of the observation noise variance r^o. The filter parameters are here the same as those used for generating the truth signal; the filter suite is described in Section 3.

Column 1 of Fig. 6 illustrates filtering with correct parameters in all filters; columns 2 and 3 show results of filtering with, respectively, overestimated and underestimated decorrelation time the hidden damping fluctuations $\gamma(t)$.

Filtering skill in regime I as a function of filter parameters (Fig. 7)

Fig. 7 summarizes the performance of imperfect filters using moment closure (GCF, DMF) and tangent (SDMF, TEKF) approximations with additional model error due to incorrect filter parameters. The most interesting effects arise due to incorrect noise amplitudes, σ_γ^M and σ_u^M, assumed by the filters in the dynamics of the resolved variable u and the unresolved

Please cite this article in press as: M. Branicki et al., Filtering skill for turbulent signals for a suite of nonlinear and linear extended Kalman filters, J. Comput. Phys. (2011), doi:10.1016/j.jcp.2011.10.029

Regime II. Filtering with correct parameter values in **INTERVAL 3**.

The mean stability parameter: $\chi = -0.05$ (weakly damped dynamics of u).
Decorrelation time of u: $1/\hat{\gamma} \approx 1.81$
Observation time: Δt^{obs} varied
True signal parameters: $\hat{\gamma} = 0.55, d_\gamma = 0.5, \sigma_\gamma = 0.5, \quad \omega_u = 1.78, \sigma_u = 0.1, \quad \gamma_b = 0.4, \omega_b = 1, \sigma_b = 0.4.$
Observation error: $\sqrt{r^o} = 0.44.$

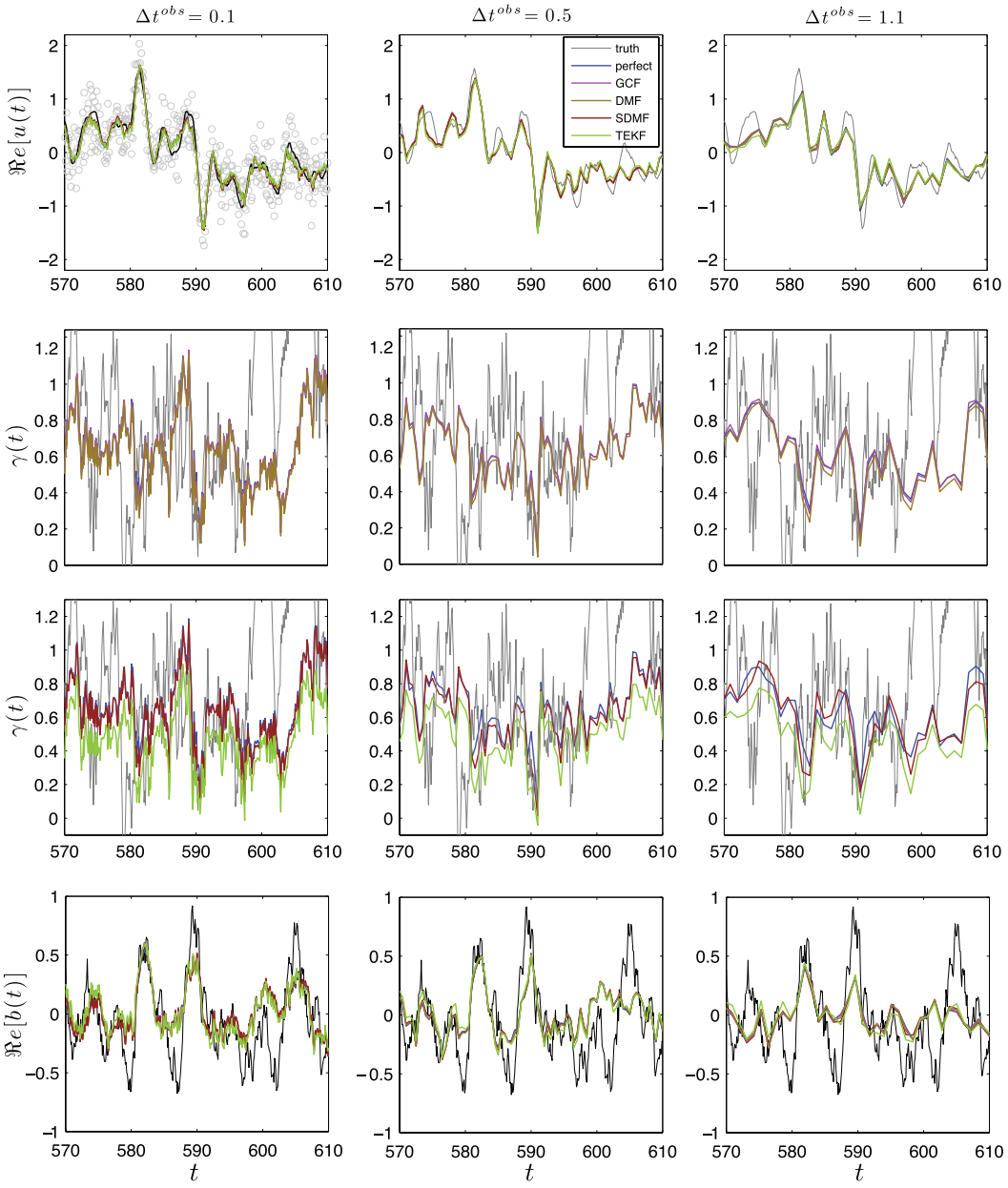

Fig. 10. (Regime II). Path-wise example of filtering within interval 2 (see Fig. 8) for three different observation times, Δt^{obs}, and a fixed value of the observation noise variance r^o. The filter parameters are here the same as those used for generating the truth signal; the filter suite is described in Section 3.

damping fluctuations γ, and due to incorrect decorrelation time $1/d_\gamma^M$ of $\gamma(t)$. The decorrelation time of the truth signal $u(t)$ in the tests is approximately $1/\hat{\gamma} = 0.8$. Each test is carried out for four different pairs of fixed values of the observation time Δt^{obs} and observation noise variance r^o. The chosen time steps are such that $\Delta t^{obs} = 0.1$ is much shorter and $\Delta t^{obs} = 0.6$ is comparable with the decorrelation time of u. The observation noise variances are chosen such that $r^o = 0.05$ corresponds to large signal-to-noise levels and $r^o = 0.5$ corresponds to moderate noise values.

Please cite this article in press as: M. Branicki et al., Filtering skill for turbulent signals for a suite of nonlinear and linear extended Kalman filters, J. Comput. Phys. (2011), doi:10.1016/j.jcp.2011.10.029

Regime II. Filtering skill as a function of the observation noise variance.

The mean stability parameter: $\chi = -0.05$.
Decorrelation time of u: $1/\hat{\gamma} \approx 1.81$
True signal parameters: $\hat{\gamma} = 0.55, d_\gamma = 0.5, \sigma_\gamma = 0.5, \quad \omega_u = 1.78, \sigma_u = 0.1, \quad \gamma_b = 0.4, \omega_b = 1, \sigma_b = 0.4.$
Incorrect filter parameters: $\sigma_u^M = 0.2$ and (Column 2) $d_\gamma^M = 0.35$, $\sigma_\gamma^M = 0.55$, (Column 3) $d_\gamma^M = 0.6$, $\sigma_\gamma^M = 0.4$,

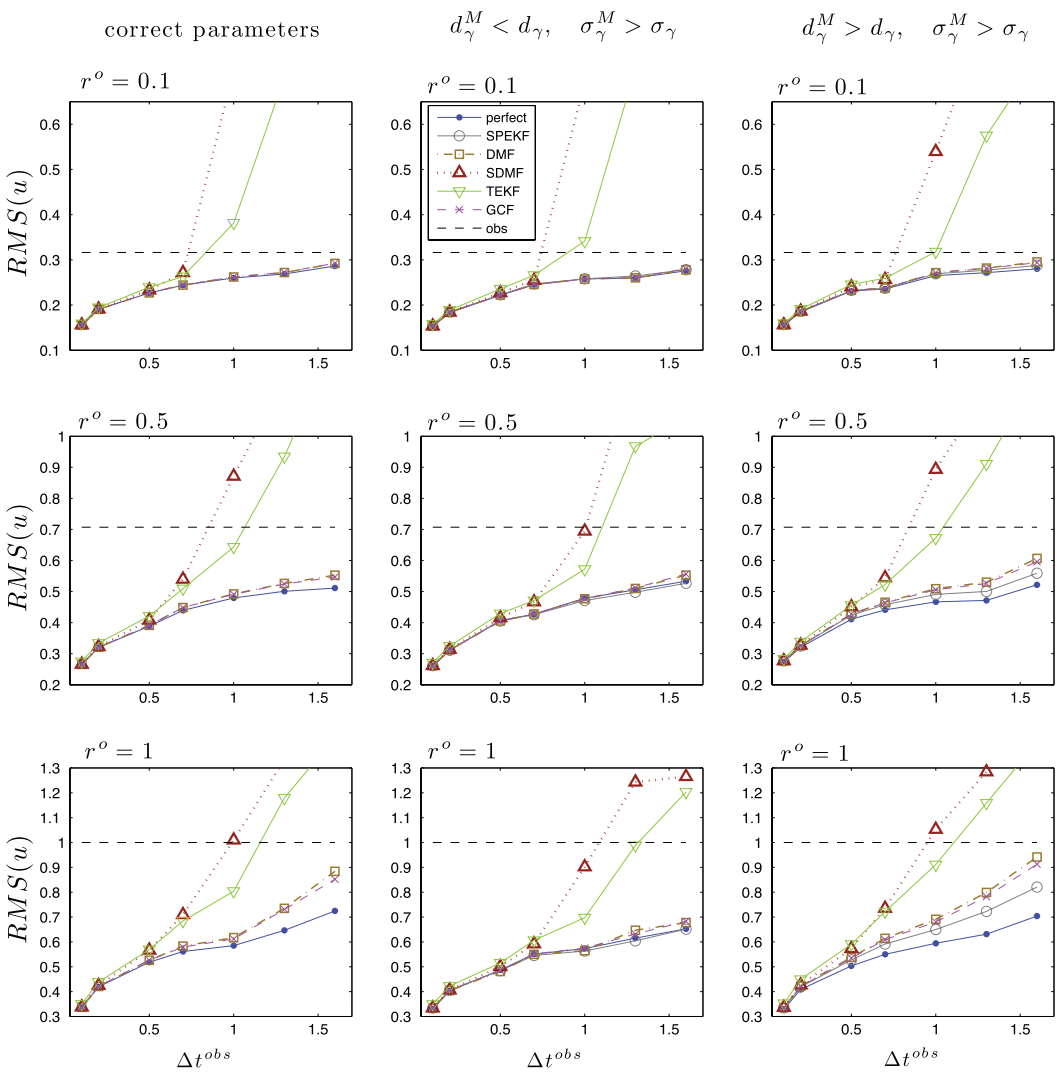

Fig. 11. (Regime II) Average RMS errors of the filtered solution $u(t)$ as a function of the observation time step Δt^{obs} for fixed values of the observation noise variance r^o and different filter parameters. For $r^o \gtrsim 1$ the signal is dominated by noise. The filter suite is described in Section 3.

8. Filter performance and parameter estimation skill in regime of intermittent large bursts of instability (Regime II)

8.1. Characteristics of the filtered signal

This configuration corresponds to regime II of mean-stable dynamics of the system (1) discussed in Section 2.1. Here, the damping d_γ in the dynamics of the hidden damping fluctuations $\gamma(t)$ is much weaker than in regime I. Consequently, the intermittent phases of transient instabilities are less frequent here but they are, on average, longer lasting than in regime I. Corresponding path-wise solutions are characterized by intermittent, large amplitude bursts of instability separated by quiescent periods dominated by a low-frequency modulation due to the deterministic forcing (see Fig. 8).

In this regime the decorrelation time of fluctuations in $\gamma(t)$, given by $1/d_\gamma$, is much longer than in regime I but the mean damping, $\hat{\gamma}$, and decorrelation time, $1/\hat{\gamma}$, of fluctuations in $u(t)$ can vary widely as in regime I, as long as $\chi < 0$. The resulting dynamics can be roughly divided into three subcategories according to the strength of the mean damping $\hat{\gamma}$: (i) Strongly damped dynamics and short decorrelation times of fluctuations in $u(t)$, i.e., $\hat{\gamma} \gg 1$, (ii) Weakly damped dynamics of and long decorrelation times of fluctuations in $u(t)$, i.e., $0 < \hat{\gamma} < 1$, (iii) Moderately damped dynamics and moderate decorrelation times of fluctuations in $u(t)$, i.e., $\hat{\gamma} \sim 1$.

Please cite this article in press as: M. Branicki et al., Filtering skill for turbulent signals for a suite of nonlinear and linear extended Kalman filters, J. Comput. Phys. (2011), doi:10.1016/j.jcp.2011.10.029

Regime II. Filtering with correct parameter values within different intervals.

The mean stability parameter: $\chi = -0.05$ (weakly damped dynamics of u).
Decorrelation time of u: $1/\hat{\gamma} \approx 1.81$
Observation time: Δt^{obs} varied
True signal parameters: $\hat{\gamma} = 0.55, d_\gamma = 0.5, \sigma_\gamma = 0.5, \quad \omega_u = 1.78, \sigma_u = 0.1, \quad \gamma_b = 0.4, \omega_b = 1, \sigma_b = 0.1.$
Observation error: $\sqrt{r^o}$ varied.

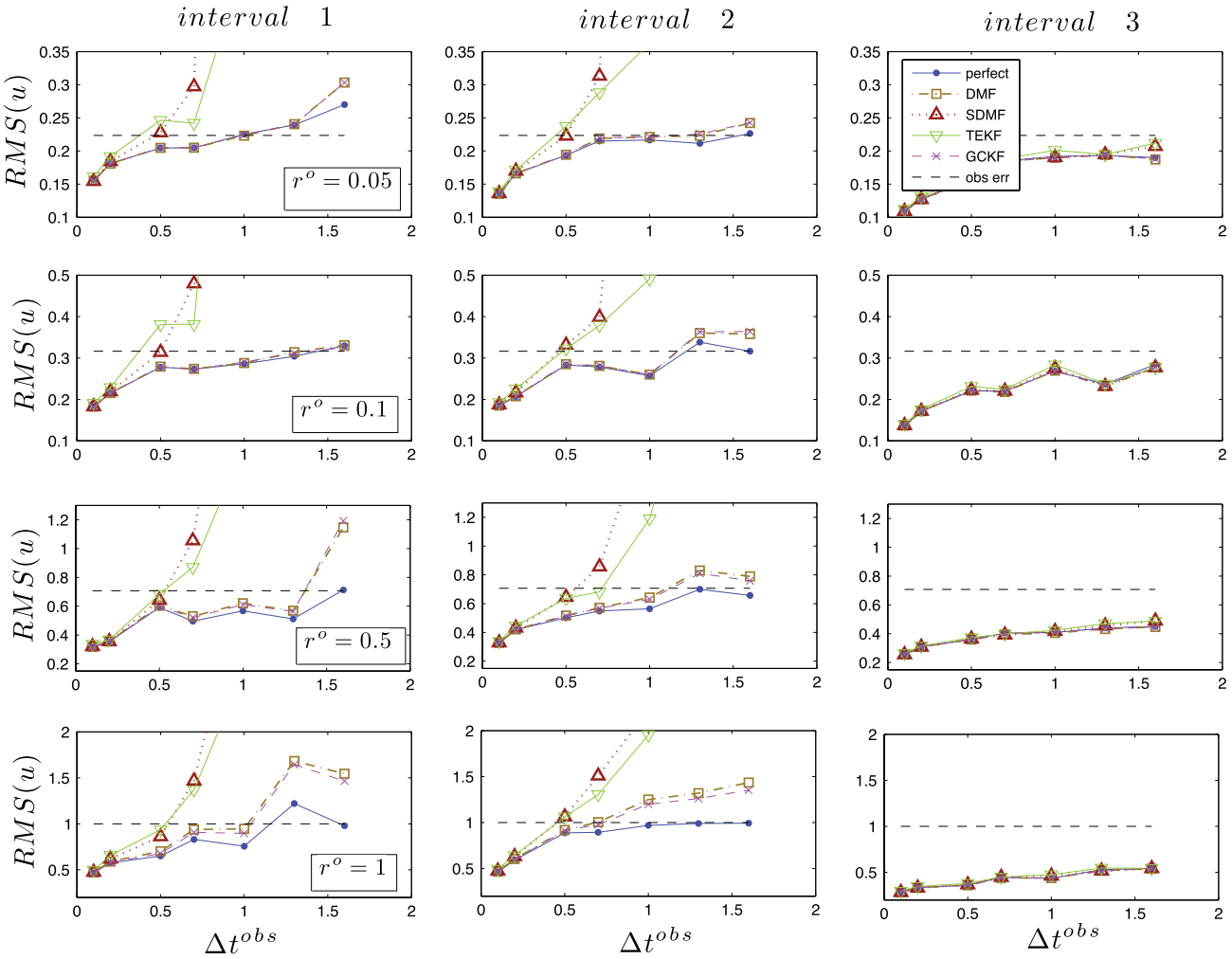

Fig. 12. (Regime II) Filtering with correct parameter values. Average RMS errors of $u(t)$ as a function of the observation time Δt^{obs} for fixed true signal and fixed values of the observation noise variance r^o. Columns show the RMS errors in the three intervals shown in Fig. 8. The filter suite is described in Section 3.

In the filtering tests carried out in this section we have chosen true signals obtained from (1) with weakly damped dynamics so that the low frequency modulation is interleaved with intermittent, large-amplitude unstable bursts in $u(t)$. For moderate and strong damping strengths in $u(t)$ the signals are too similar to those discussed in regime I.

In all simulations carried out in this section the true signal is generated from (1) with parameters

$$\hat{\gamma} = 0.55, d_\gamma = 0.5, \sigma_\gamma = 0.5, \quad \omega_u = 1.78, \sigma_u = 0.4, \gamma_b = 0.4, \omega_b = 1, \sigma_b = 0.4, \tag{30}$$

so that the mean stability parameter is $\chi = -0.05$.

Path-wise solutions of (1) in regime II are characterized by drastically different dynamical phases. Consequently, the RMS errors averaged over the whole observation interval do not provide a sufficiently detailed diagnostics of filter performance. Therefore, we focus here on three distinct intervals of our truth signal (see Fig. 8):

Interval 1 with a large-amplitude transient instability in $u(t)$ which dominates the low-frequency modulation due to the deterministic forcing.

Interval 2 with two successive instabilities in $u(t)$. Here, the two intervals where $\gamma(t) < 0$ occur in a short succession so that the first unstable burst is not completely damped before the next one occurs. This is a tough test for any filter since there is not enough observations between the two unstable events to predict the second transient instability in the signal.

Please cite this article in press as: M. Branicki et al., Filtering skill for turbulent signals for a suite of nonlinear and linear extended Kalman filters, J. Comput. Phys. (2011), doi:10.1016/j.jcp.2011.10.029

Interval 3 - Quiescent phase. The low-frequency modulation of the signal is accompanied by short, isolated, small-amplitude instabilities.

8.2. Filtering with imperfect models

Here, we summarize the most important characteristics of filtering with imperfect models in regime II (cf. Section 2.1). Properties of filtering with the perfect filter in this regime were discussed in Section 5 (see Cases 1–4). A more detailed discussion of the filter skill and a description of accompanying figures are presented in Section 8.2.1.

Filtering skill in regime II:

- In regime II the skill hierarchy of the analyzed filters is

  $SPEKF \sim GCF \sim DMF \gg SDMF \sim TEKF$

Regime II. Filtering skill as a function of observation noise variance.

The mean stability parameter: $\chi = -0.05$.
Decorrelation time of u: $1/\hat{\gamma} \approx 1.81$
True signal parameters: $\hat{\gamma} = 0.55, d_\gamma = 0.5, \sigma_\gamma = 0.5, \quad \omega_u = 1.78, \sigma_u = 0.1, \quad \gamma_b = 0.4, \omega_b = 1, \sigma_b = 0.4.$
Incorrect filter parameters: $\sigma_u^M = 0.2$, (Column 2) $d_\gamma^M = 0.35$, $\sigma_\gamma^M = 0.55$, (Column 3) $d_\gamma^M = 0.6$, $\sigma_\gamma^M = 0.4$,

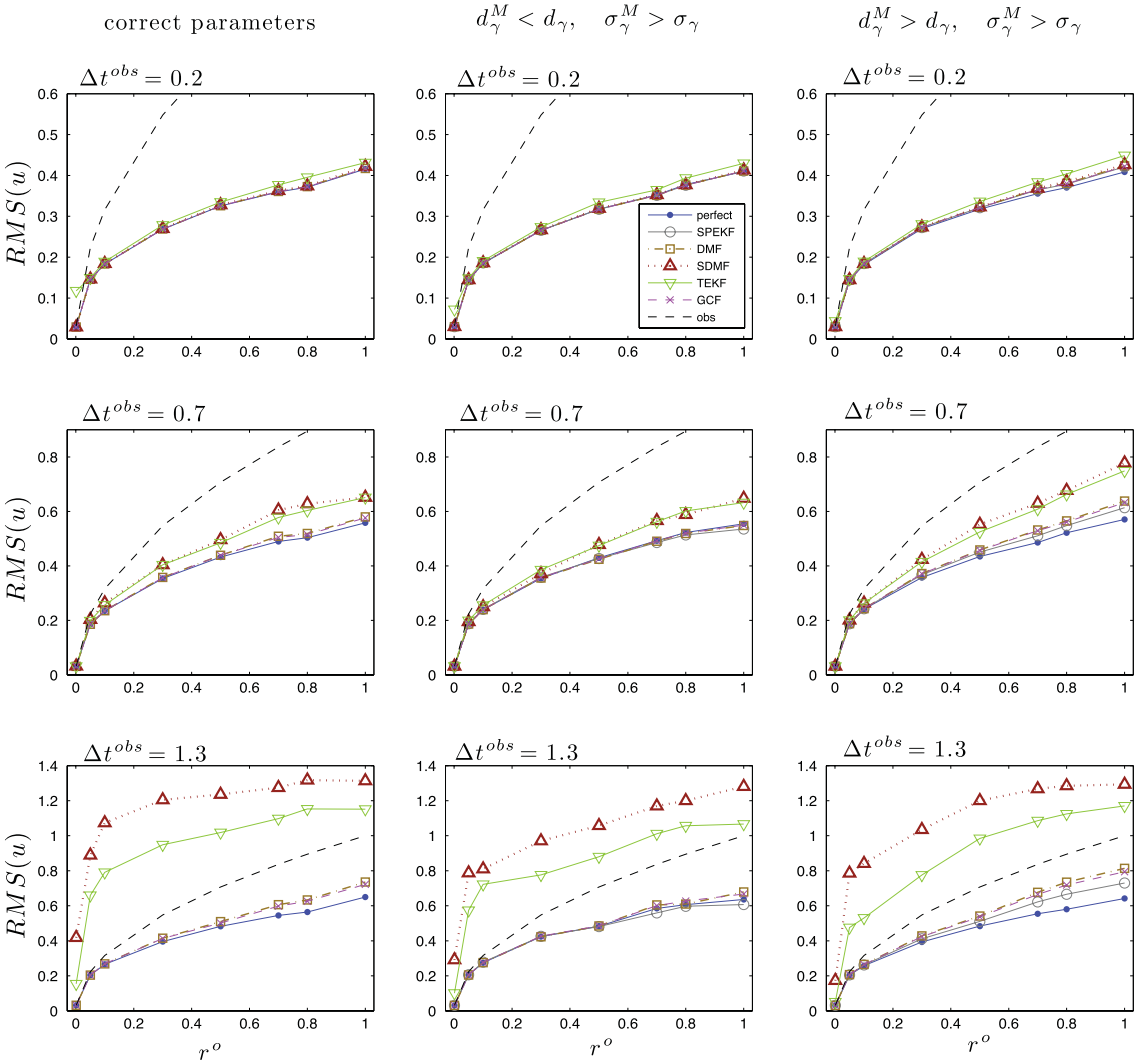

Fig. 13. (Regime II) Average RMS errors of the filtered solution $u(t)$ as a function of the observation noise variance r^o for fixed values of the observation time step Δt^{obs} and different filter parameters. For $r^o \gtrsim 1$ the signal is dominated by noise. The filter suite is described in Section 3.

Please cite this article in press as: M. Branicki et al., Filtering skill for turbulent signals for a suite of nonlinear and linear extended Kalman filters, J. Comput. Phys. (2011), doi:10.1016/j.jcp.2011.10.029

Regime II. Filtering with imperfect models.

The mean stability parameter: $\chi = -0.05$.
Decorrelation time of u: $1/\hat{\gamma} \approx 1.81$
True signal parameters: $\hat{\gamma} = 0.55, d_\gamma = 0.5, \sigma_\gamma = 0.5, \quad \omega_u = 1.78, \sigma_u = 0.1, \quad \gamma_b = 0.4, \omega_b = 1, \sigma_b = 0.4.$
Incorrect filter parameters: σ_γ^M, d_γ^M, σ_u^M varied.

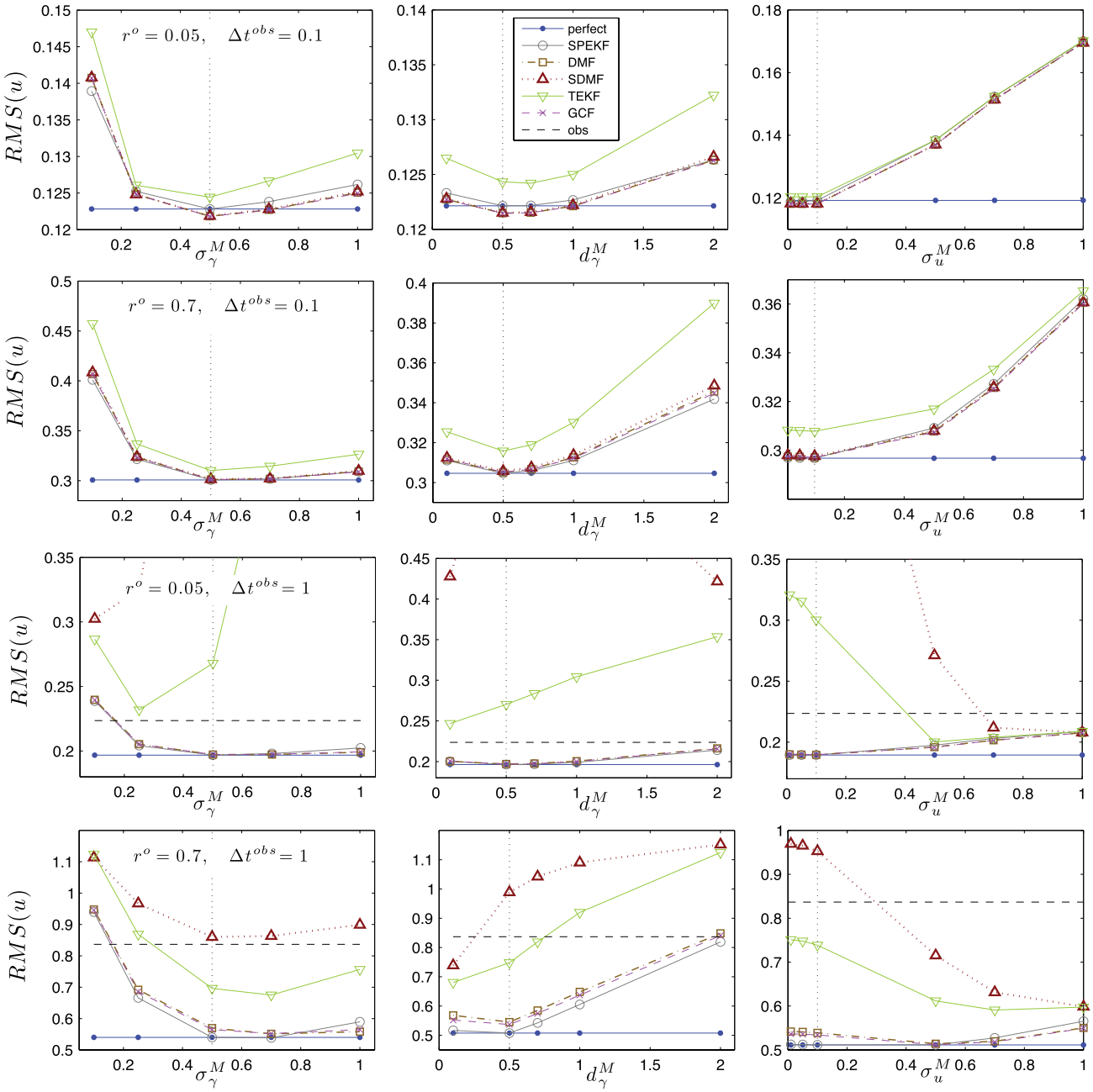

Fig. 14. (Regime II) Filtering with imperfect models (cf Section 6). Average RMS errors of the filtered signal $u(t)$ as a function of the filter parameter σ_γ^M (incorrect noise amplitude assumed for $\gamma(t)$) for fixed values of the observation time Δt^{obs} and fixed observation noise variance r^o. The filter suite is described in Section 3.

The differences in filter skill increase monotonically with the observation time, Δt^{obs}, and observation noise variance, r^o, but this hierarchy remains unchanged (Figs. 11–13) and is also largely insensitive to errors in the filter parameters.

- TEKF and SDMF are completely unreliable in this regime and they diverge even for correct parameter values due to their failure in predicting the intermittent, large-amplitude unstable events in the dynamics of $u(t)$ (Figs. 9 and 12); these filters often produce erroneous super-stable phases ($\gamma^M(t) \gg 1$) in regions of transient instability in the true signal, i.e. when

Please cite this article in press as: M. Branicki et al., Filtering skill for turbulent signals for a suite of nonlinear and linear extended Kalman filters, J. Comput. Phys. (2011), doi:10.1016/j.jcp.2011.10.029

$\gamma(t) < 0$ (Fig. 9). The performance of SDMF and TEKF is only satisfactory in the quiescent intervals in which all filters have a good and comparable skill (see Figs. 12 and 10).

- The skill of SPEKF, GCF and DMF remains good for overestimated decorrelation time of γ (i.e., when $d_\gamma^M \leqslant d_\gamma$) and it somewhat deteriorates for underestimated decorrelation time of the hidden damping fluctuations γ; however, even in extreme cases these filters outperform TEKF and SDMF (Fig. 14).
- The largest skill differences between the examined filters occur when filtering with large observation times ($\Delta t^{obs} \sim 1/\hat{\gamma}$) within intervals associated with large-amplitude intermittent instabilities (Fig. 12).
- The moment closure errors due to neglecting the third moments in the model covariance evolution (16b) dominate the errors due to neglecting the second moments in the model mean evolution (16a) (see GCF, DMF and SPEKF (perfect filter) in Figs. 11, 12 and compare with Figs. 14 and 7).
- The skill of all filters deteriorates for underestimated noise amplitude σ_γ^M in γ (Fig. 14), or for severely underestimated decorrelation time of γ (see Fig. 14 for $d_\gamma^M \gg d_\gamma$). The filtering skill in this regime can also be significantly affected by insufficient resolution of the short, large-amplitude unstable bursts in the truth signal (Fig. 9).

Regime II. Parameter estimation.

The mean stability parameter: $\chi = -0.05$ (weakly damped dynamics of u).
Decorrelation time of u: $1/\hat{\gamma} \approx 1.81$
Observation time: Δt^{obs} varied
True signal parameters: $\hat{\gamma} = 0.55, d_\gamma = 0.5, \sigma_\gamma = 0.5, \quad \omega_u = 1.78, \sigma_u = 0.1, \quad \gamma_b = 0.4, \omega_b = 1, \sigma_b = 0.1.$
Filter parameters: all correct
Observation error: $\sqrt{r^o}$ varied.

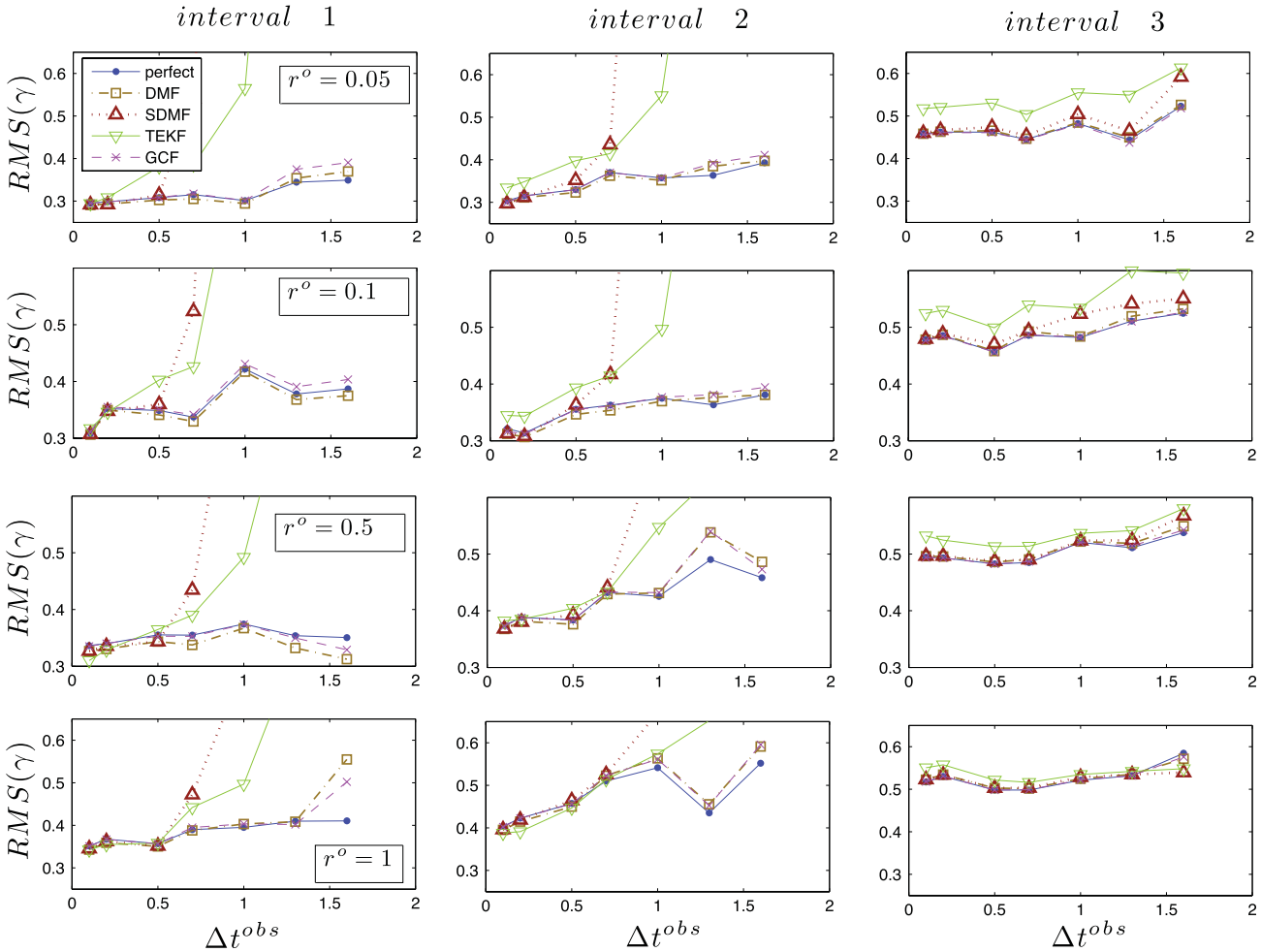

Fig. 15. (Regime II) Parameter estimation. Average RMS errors of $\gamma(t)$ as a function of the observation time Δt^{obs} for fixed true signal and fixed values of the observation noise variance r^o. Columns show the RMS errors in the three intervals shown in Fig. 8. The filter suite is described in Section 3.

Please cite this article in press as: M. Branicki et al., Filtering skill for turbulent signals for a suite of nonlinear and linear extended Kalman filters, J. Comput. Phys. (2011), doi:10.1016/j.jcp.2011.10.029

Regime II. Filtering with correct parameter values.

The mean stability parameter: $\chi = -0.05$ (weakly damped dynamics of u).
Decorrelation time of u: $1/\hat{\gamma} \approx 1.81$
Observation time: Δt^{obs} varied
True signal parameters: $\hat{\gamma} = 0.55, d_\gamma = 0.5, \sigma_\gamma = 0.5, \quad \omega_u = 1.78, \sigma_u = 0.1, \quad \gamma_b = 0.4, \omega_b = 1, \sigma_b = 0.1.$
Filter parameters: all correct
Observation error: $\sqrt{r^o}$ varied.

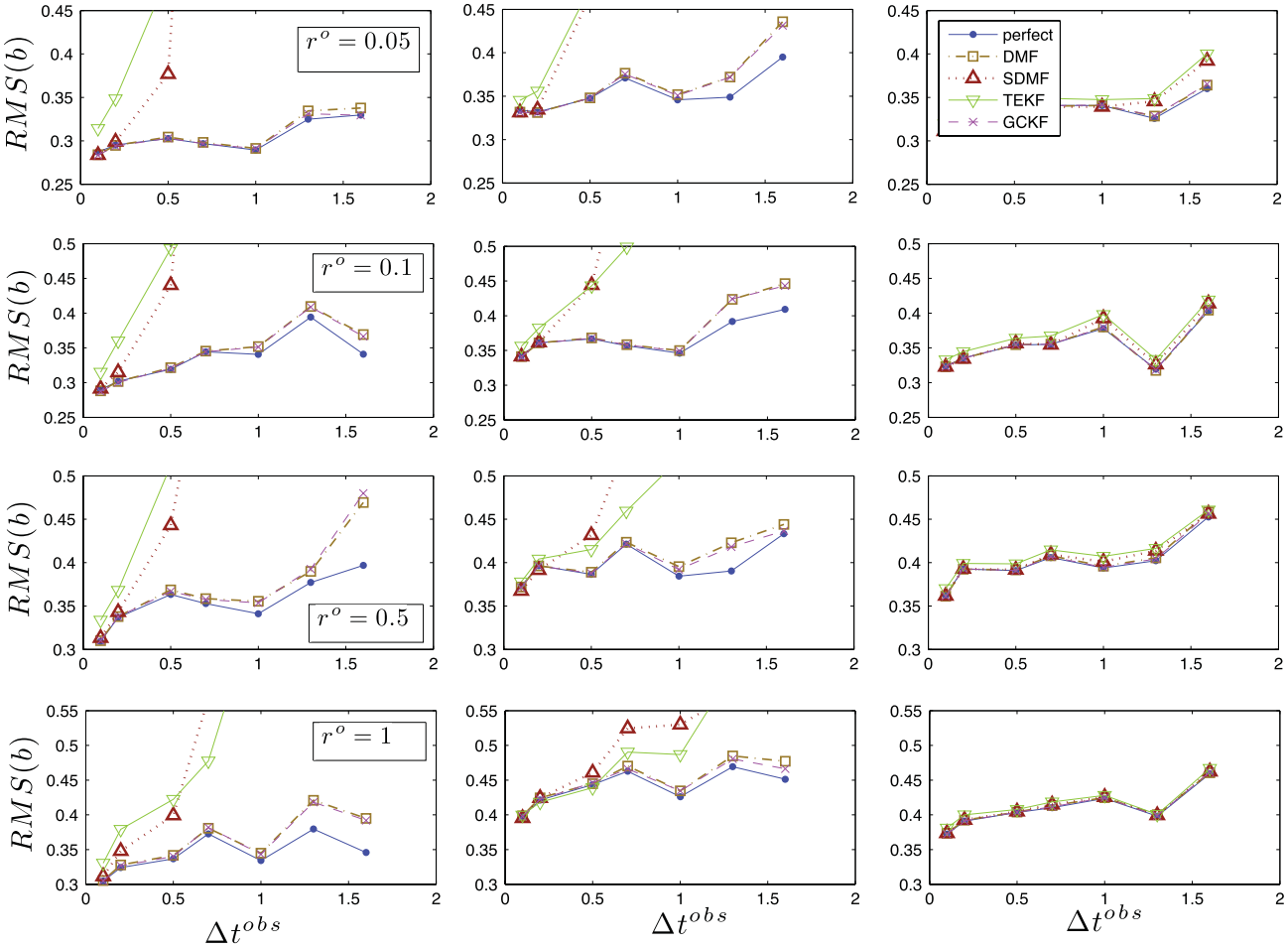

Fig. 16. (Regime II) Parameter estimation. Average RMS errors of $b(t)$ as a function of the observation time Δt^{obs} for fixed true signal and fixed values of the observation noise variance r^o. Columns show the RMS errors in the three intervals shown in Fig. 8. The filter suite is described in Section 3.

Parameter estimation in regime II:

- The estimation of the stochastic damping fluctuations, $\gamma(t)$, from SPEKF, GCF and DMF is similar and it is the best in regions of intermittent instabilities when the signal-to-noise ratio is high and the filters trust the observations (Figs. 15 and 9, 10). This allows SPEKF, GCF and DMF to recover the dominant negative minima of $\gamma(t)$ (extrema of instability) resulting in a good overall skill of these filters. In quiescent intervals with no transient instabilities the estimation skill of γ deteriorates since it is not needed for high filtering skill.
- Parameter estimation by SPEKF is the least sensitive to incorrect filter parameters.
- The estimation of the hidden multiplicative and additive biases, $\gamma(t)$ and $b(t)$, by TEKF and SDMF is completely unreliable during the large-amplitude, intermittent instabilities (Figs. 9, 10 and 16). For sufficiently large observation times ($\Delta t^{obs} \sim 1/\hat{\gamma}$) these filters predict erroneous phases of strongly stable dynamics (i.e., $\gamma^M(t) \gg 1$) during unstable phases in the truth signal $\gamma(t) < 0$ (Fig. 9).
- The estimation of $b(t)$ by SPEKF, GCF and DMF is comparable in all intervals (Figs. 16 and 9, 10) and it is good provided that the observation time is shorter that the decorrelation time of $b(t)$.

Please cite this article in press as: M. Branicki et al., Filtering skill for turbulent signals for a suite of nonlinear and linear extended Kalman filters, J. Comput. Phys. (2011), doi:10.1016/j.jcp.2011.10.029

Regime III. Filtering and parameter estimation.

The mean stability parameter: $\chi = -0.1$.
Decorrelation time of u: $1/\hat{\gamma} \approx 0.12$
True signal parameters: $\hat{\gamma} = 8.1, d_\gamma = 0.25, \sigma_\gamma = 1, \quad \omega_u = 1.78, \sigma_u = 0.25, \quad \gamma_b = 0.5, \omega_b = 1, \sigma_b = 0.5.$
Incorrect filter parameters: $d_\gamma^M = 0.3.$

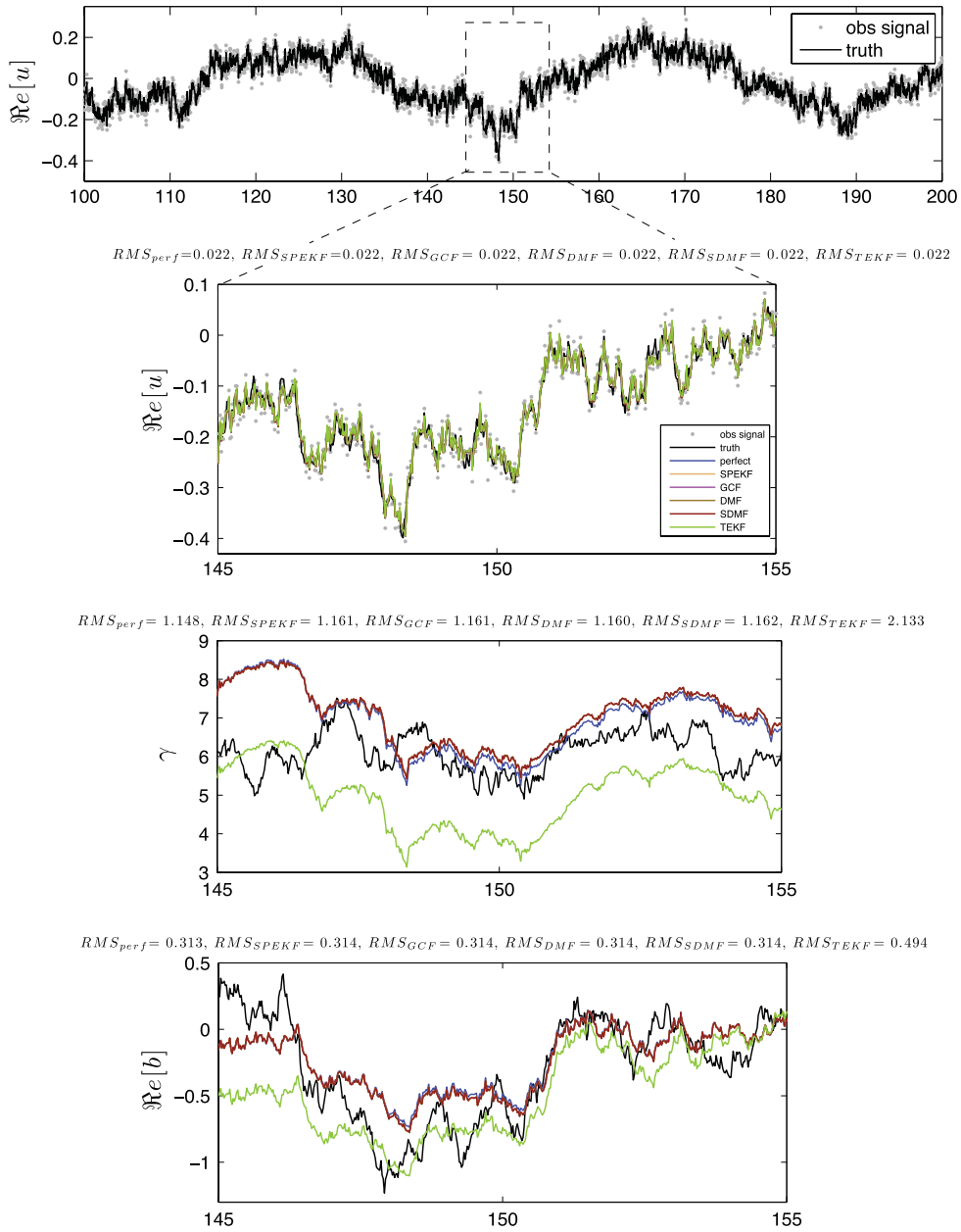

Fig. 17. (Regime III) Path-wise filtering with incorrect parameters (cf. Section 6) when the decorrelation time of fluctuations in $\gamma(t)$ assumed in the filters is underestimated (i.e., $d_\gamma^M > d_\gamma$). The filter suite is described in Section 3.

8.2.1. Specific examples

We provide here more details on the performance of different filters for different observation times, observation noise variances and incorrect parameter values used in the filters from our suite (cf. Section 3). Properties of filtering with the perfect filter in this regime, which is used as a benchmark here, were discussed in Section 5 (see Cases 1–4).

Path-wise examples of filtering in regime II (Figs. 8,9,10)

In Figs. 8–10 we show three path-wise examples of filtering in regime II; all of them for correct filter parameters. Fig. 8 illustrates filtering and parameter estimation using the perfect filter which is given by SPEKF with correct parameter values. The observed signal $u(t)$ is filtered in the presence of moderate observation noise variance, r^o, and the observation time step, Δt^{obs}, which is much shorter than the decorrelation times of u,γ and b in (1). The outcome of the filtering in the three

Please cite this article in press as: M. Branicki et al., Filtering skill for turbulent signals for a suite of nonlinear and linear extended Kalman filters, J. Comput. Phys. (2011), doi:10.1016/j.jcp.2011.10.029

Regime III. Parameter estimation with imperfect models.

The mean stability parameter: $\chi = -0.1$.
Decorrelation time of u: $1/\hat{\gamma} \approx 0.12$
True signal parameters: $\hat{\gamma} = 8.1, d_\gamma = 0.25, \sigma_\gamma = 1, \quad \omega_u = 1.78, \sigma_u = 0.25, \quad \gamma_b = 0.5, \omega_b = 1, \sigma_b = 0.5.$
Incorrect forecast model parameters: $\sigma_\gamma^M, d_\gamma^M, \sigma_u^M$ varied.
Observation time: $\Delta t^{obs} = 0.08$
Observation noise variance: $r^o = 0.0008$

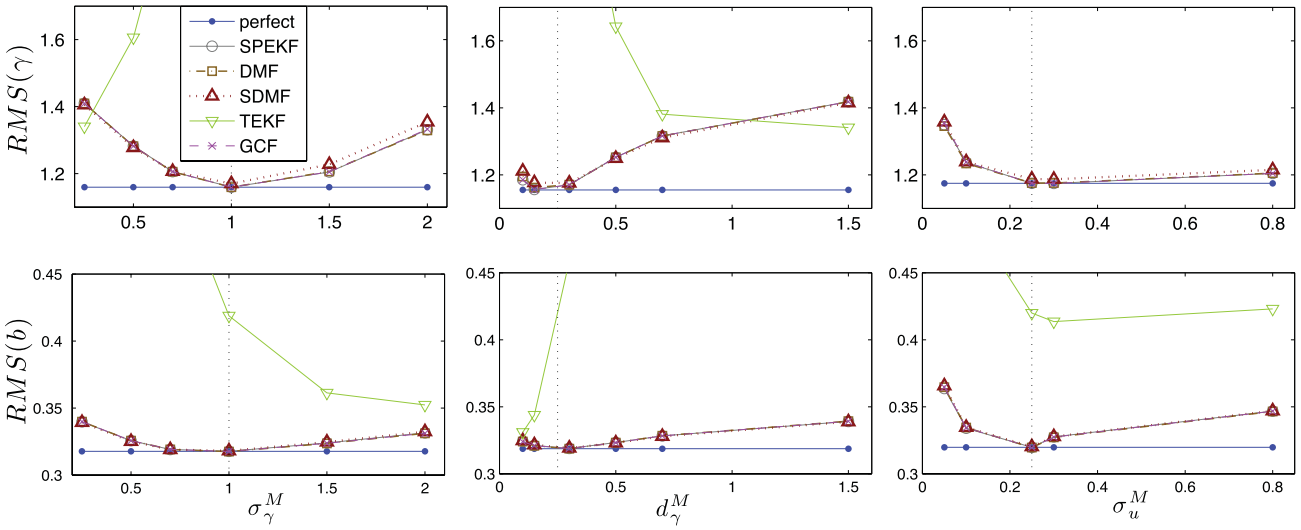

Fig. 18. (Regime III) Parameter estimation with imperfect models (see Section 3). Average RMS errors for the stochastic parameters γ and b in the augmented forecast model (1) estimated from the observations of $u(t)$ as a function of the filter noise amplitudes $\sigma_\gamma^M, \sigma_u^M$ and decorrelation time, $1/d_\gamma^M$, of $\gamma^M(t)$; the correct parameter values are marked by the dotted vertical lines. The results are largely independent of the observation time Δt^{obs} and observation noise variance r^o within the intervals $0 \lesssim \Delta t^{obs} \lesssim 0.1$ and $0 \lesssim r^o \lesssim 0.001$.

intervals described in Section 8 is shown in separate insets. The filtering skill of the observed variable, $u(t)$, is good in all three intervals. The dynamics of the hidden damping fluctuations, $\gamma(t)$, is estimated much better in the intervals 1 and 2 than in the quiescent interval 3. In particular, the extrema of instability (i.e. negative minima of $\gamma(t)$) are well detected in interval 1; as in regime I this feature is crucial for a skillful filtering of $u(t)$.

Figs. 9 and 10 show path-wise examples of filtering with imperfect filters in intervals 1 and 3 (cf. Section 8). Fig. 3 shows examples of filtering with correct parameters for three different observation time steps. SPEKF, GCF and DMF clearly outperform TEKF and SDMF in interval 1 which contains a large-amplitude burst of transient instability. The dominant minima of γ are well detected by SPEKF, GCF and DMF. When filtering with large observation time steps, the filtering skill of all filters is affected by insufficient resolution of the unstable bursts in the observed signal. SPEKF, GCF and DMF remain more skillful than SDMF and TEKF; in fact, TEKF and SDMF erroneously predict phases of strong stability in regions of transient instability in the truth signal. The skill differences in quiescent regions are much less pronounced, as illustrated in Fig. 10.

Filtering skill in regime II as a function of the observation time step (Figs. 11 and 12)

In Figs. 11 and 12 we show the average RMS errors of the filtered solutions $u(t)$ as a function of the observation time step, Δt^{obs}, for different, fixed values of the observation variance, r^o, and various combinations of the filter parameters. The filtering procedure is performed by sampling the same truth signal, generated from (1) with parameters (30), with different observation times. The chosen values of the observation noise variance, r^o, are such that the smallest considered value, $r^o = 0.01$, corresponds to high overall signal-to-noise ratio, while for $r^o = 2$ the signal is dominated by the observation noise. In the first column of Fig. 11 correct parameter values are used in all filters so that the model errors are only due to the incorrect statistics. Columns 2 and 3 of Fig. 11 illustrate filtering with incorrect parameter values which introduces an additional model error and gives some indication of the importance of the errors due to incorrect statistics. In column 2 the of Fig. 11 all filters overestimate the decorrelation time of the unresolved variable γ (i.e., $d_\gamma^M < d_\gamma$); in column 3 all filters underestimate the decorrelation time of γ (i.e., $d_\gamma^M > d_\gamma$).

Filtering skill in regime II as a function of the observation noise variance (Fig. 13)

The dependence of the filtering skill on the observation noise variance, r^o, in this regime is summarized in Fig. 13 which shows the average RMS errors of the filtered signal, $u(t)$, as a function of r^o for fixed values of the observation time step, Δt^{obs}, and for various combinations of filter parameters. The same truth signal as in the previous tests was used here. Column 1 of Fig. 13 shows results of filtering with correct parameters in all filters; columns 2 and 3 show results of analogous computations with, respectively, overestimated and underestimated decorrelation time of the hidden damping fluctuations $\gamma(t)$.

Please cite this article in press as: M. Branicki et al., Filtering skill for turbulent signals for a suite of nonlinear and linear extended Kalman filters, J. Comput. Phys. (2011), doi:10.1016/j.jcp.2011.10.029

Filtering skill in regime II as a function of filter parameters (Fig. 14)

Fig. 14 summarizes the performance of imperfect filters using incorrect statistics with an additional model error due to incorrect filter parameters. As in regime I, the most interesting effects arise due to incorrect noise amplitudes σ_γ^M, σ_u^M assumed by the filters in the dynamics of the resolved variable $u(t)$ and the hidden damping fluctuations $\gamma(t)$, and due to incorrect decorrelation time $1/d_\gamma^M$ of $\gamma(t)$. The decorrelation time of the truth signal $u(t)$ in the tests is approximately $1/\hat{\gamma} = 1.8$. Each test is carried out for four different pairs of fixed values of the observation time $\Delta\, t^{obs}$ and observation noise variance r^o. The chosen time steps are such that $\Delta t^{obs} = 0.1$ is much shorter and $\Delta\, t^{obs} = 1$ is comparable with the decorrelation time of u. The observation noise variances are chosen such that $r^o = 0.05$ corresponds to large overall signal-to-noise levels in the quiescent interval 3 and $r^o = 0.7$ corresponds to moderate noise values.

Estimation of $\gamma(t)$ and $b(t)$ in regime II (Figs. 15 and 16)

Figs. 15 and 16 illustrate typical characteristics of estimation of the stochastic parameters γ and b whose dynamics in the augmented forecast model (1) is hidden from observations. Fig. 15 shows the RMS errors of $\gamma(t)$ within the intervals 1–3 discussed earlier (see Fig. 8) as a function of the observation time step Δt^{obs} and for different fixed values of the observation noise variance r^o; the observation noise variances were chosen such that $r^o = 0.05$ corresponds to large signal-to-noise ratio in the quiescent interval 3 and for $r^o = 1$ the signal is dominated by noise in interval 3; note that due to the large amplitude of the unstable burst in interval 1, the signal-to-noise ratio in this interval remains large for both noise levels. Fig. 16 shows the RMS errors of $b(t)$ within the three distinct intervals discussed earlier (see Fig. 8) as a function of the observation time step and for different fixed values of the observation noise variance r^o.

9. Parameter estimation in the laminar regime (Regime III)

In this nearly Gaussian regime the filtering skill of all filters is comparable and good, and we mostly focus on the estimation skill of the stochastic parameters γ and b whose augmented dynamics in the test model (1) is hidden from observations.

9.1. Characteristics of the filtered signal

This configuration corresponds to regime III of mean-stable dynamics of the system (1) which was identified in Section 2.1. Signals in this regime are characterized by long decorrelation times of fluctuations in γ (in the sense that $d_\gamma \ll \sigma_\gamma, \sigma_\gamma \sim \mathcal{O}(1)$) and a rapidly decorrelating fluctuations in the observed component $u(t)$ (i.e., $1/\hat{\gamma} \ll 1$). Thus, the corresponding path-wise solutions of (1) are dominated by low frequency modulation due to the deterministic forcing with superimposed small-amplitude fluctuations. Transient instabilities are very rare in this configuration but they can have very large amplitudes.

In the numerical tests we have chosen the truth signals generated from (1) with parameters

$$\hat{\gamma} = 8.1, d_\gamma = 0.25, \sigma_\gamma = 1, \quad \omega_u = 1.78, \sigma_u = 0.25, \gamma_b = 0.5, \omega_b = 1, \sigma_b = 0.5; \tag{31}$$

see Fig. 17 for a path-wise example of solution generated with these parameters. In this configuration the observed component $u(t)$ decorrelates much faster than $\gamma(t)$. For parameters (31) the decorrelation time of u is approximately $1/\hat{\gamma} \approx 0.12$, the decorrelation time of γ is $1/d_\gamma = 4$ and the mean stability parameter is $\chi = -0.1$.

9.2. Filtering with imperfect models

Below, we summarize the most important characteristics of filtering and parameter estimation in regime III. Properties of filtering with a perfect filter in regime III, which is used as a benchmark here, were discussed in Section 5 (see Cases 2–4).

Filter performance in regime III:

- The filtering skill for all filters is comparable and good except for large observation times, $\Delta t^{obs} \sim 1/\hat{\gamma}$, and small observation noise levels (not shown).
- The effects of model error due to different moment closure approximations are insignificant in this regime.

Parameter estimation in regime III (Fig. 18):

- The estimation of the hidden damping fluctuations $\gamma(t)$ from SPEKF, GCF, DMF and SDMF is similar and comparable with the perfect filter when filtering with correct parameters. The model error due to various moment closures has no discernible effect on parameter estimation in this regime.
- The mean value of $\gamma(t)$ is recovered well, except for large observation times, $\Delta t^{obs} \sim 1/\hat{\gamma}$. There are essentially no transient instabilities in this regime and a good estimate of the mean leads to a high skill of the filtered solution $u(t)$.
- TEKF is completely unreliable at estimating γ and b. TEKF is also very sensitive to incorrect filter parameters.
- The parameter estimation by SPEKF, GCF, DMF and SDMF is largely insensitive to variations in filter parameters.
- $b(t)$ is recovered well by SPEKF, GCF, DMF and SDMF provided that it decorrelates sufficiently slowly, i.e., $1/\gamma_b > \Delta\, t^{obs}$.

Please cite this article in press as: M. Branicki et al., Filtering skill for turbulent signals for a suite of nonlinear and linear extended Kalman filters, J. Comput. Phys. (2011), doi:10.1016/j.jcp.2011.10.029

9.2.1. Specific examples

We only briefly discuss the results of specific tests illustrating the filtering skill as a function of the observation time step, observation noise variance, and incorrect filter parameters.

Filtering skill in regime III as a function of observation time step

The filtering skill for all filters is comparable and good except for large observation times, $\Delta t^{obs} \sim 1/\hat{\gamma}$, and small observation noise levels. These results are not illustrated here.

Parameter estimation in regime III

Fig. 18 shows the average RMS errors for the hidden stochastic parameters γ and b estimated from the augmented nonlinear forecast model (1) based on the observations of $u(t)$. The estimation skill is examined as a function of the noise amplitude, σ_γ^M, and the decorrelation time, $1/d_\gamma^M$, of the damping fluctuations $\gamma(t)$ in the augmented forecast model; the correct parameter values are indicated by dashed vertical lines. The decorrelation time of the truth signal $u(t)$ used in the tests is approximately $1/\hat{\gamma} = 0.12$. The results shown were obtained for $\Delta t^{obs} = 0.08$, which is comparable with the decorrelation time of u, and $r^o = 0.0008$ which corresponds to moderate noise levels for the system parameters (31) used in the simulations. The changes in estimation skill for $\gamma(t)$ for other observation time steps and observation noise levels are remarkably insignificant.

10. Concluding discussion and future directions

We have tested the performance of a suite of nonlinear algorithms based on state space augmentation and stochastic parameter estimation for filtering multiscale turbulent signals. The examined algorithms use the same stochastic forecast model but they implement different moment closure approximations when propagating the second-order statistics in the Kalman filtering procedure. In the set of tests aimed at understanding the effects of errors due to various moment closures the Stochastic Parameterization Extended Kalman Filter (SPEKF), involving exact formulas for updating the mean and covariance of the augmented system, was used as a benchmark and the perfect filter when filtering with correct model parameters. The remaining filters introduced additional model error through the use of incorrect statistics. A comprehensive study was presented of the filter performance in the presence of model error and within a broad range of turbulent dynamical regimes for various combinations of the observation time step and observation noise levels. The non-Gaussian test forecast model used in the analysis is nonlinear in the augmented variables and chosen in such a way as to allow for analytical tractability combined with rich dynamics mimicking various modes in the turbulent spectrum, ranging from signals with intermittent bursts of instability and positive finite-time Lyapunov exponents to laminar behavior. The following two sources of model error were considered:

(1) *Incorrect statistics* used in the filters due to particular moment closure approximations.
(2) *Incorrect parameters in the forecast models used for filtering*, assuming a perfect structure of the model.

In order to disentangle these two sources of errors, the synthetic "truth" signal was generated using the same test model as the one used for filtering but with possibly different parameters. This framework allowed for assessing the effects of errors due to incorrect statistics and their relative importance by carrying out the following tests:

(1) *Filtering with correctly specified parameters in the model*. In this case the effects of model error on filtering which arise solely from the incorrect statistics could be examined.
(2) *Filtering with incorrectly specified filter parameters*. This configuration was used to assess the robustness and importance of errors due to incorrect statistics by considering additional simple model error arising from imperfect parameters in a structurally perfect forecast model.

The true dynamics of the stochastic parameters in the augmented nonlinear forecast model, i.e., the multiplicative damping fluctuations $\gamma(t)$ and the additive forcing fluctuations $b(t)$, were known but hidden from observations. Consequently, the skill of different filters for estimating the hidden stochastic parameters from the observations of the resolved component $u(t)$ was studied by comparing the filtered solutions with the synthetic truth.

The analysis carried out here enabled a comprehensive understanding of the filtering skill and parameter estimation for various filters implementing stochastic parameter estimation and different moment closures for turbulent modes in different regimes of the turbulent spectrum. The main findings of this study are: Filtering skill:

(1) For the three examined regimes characteristic of turbulent modes in the energy transfer range (regime I - abundant transient instabilities), dissipation range (regime II - intermittent, large amplitude instabilities) and the laminar modes (regime III), the overall hierarchy of filters (from best to worst) is

$$SPEKF \gtrsim GCF \gtrsim DMF \gg SDMF \gtrsim TEKF$$

The above hierarchy suggests that the use of the tangent approximation for propagating either the prior covariance (SDMF) or both the prior covariance and the mean (TEKF) is particularly detrimental for the filtering skill.

Please cite this article in press as: M. Branicki et al., Filtering skill for turbulent signals for a suite of nonlinear and linear extended Kalman filters, J. Comput. Phys. (2011), doi:10.1016/j.jcp.2011.10.029

(2) The effects of errors due to different moment closure approximations are most pronounced in regime I where they can be comparable to imperfect model errors due to imprecise parameters. In regime I the errors due to neglecting the second moments in the model mean (DMF) are not negligible and comparable to the errors arising from neglecting the third moments in the model covariance (all imperfect filters). Neglecting the third moments in the model covariance is particularly detrimental when filtering systems with large-amplitude transient instabilities. Thus, these errors are dominant in regime II and they increase when filtering with observation times approaching the decorrelation time. In regime III the effects of incorrect filter statistics due to moment closures are insignificant and SPEKF, GCF and DFM shadow each other.
(3) TEKF and SDMF are generally unreliable. They diverge in regimes I and II for a wide range of filter parameters and observation time steps. This is mainly due to the failure of these filters to detect the intermittent, large-amplitude instabilities in the signal.
(4) Unsurprisingly, SPEKF is the most skillful filter for correct parameter values, since it is the perfect filter in such a case. SPEKF is also superior for underestimated decorrelation times of the hidden damping fluctuations $\gamma(t)$ (i.e. $d_\gamma^M \gg d_\gamma$). The performance of SPEKF is most sensitive to overestimated decorrelation time (i.e., $d_\gamma^M \ll d_\gamma$) in regime I. In regime II, SPEKF, GCF and DMF shadow each other.
(5) GCF is generally comparable to SPEKF and DMF but it performs somewhat better regime I than DMF which uses ad hoc moment closure. GCF is also the most robust filter in regime I, although SPEKF can have a better skill for underestimated decorrelation times (i.e. $d_\gamma^M \gg d_\gamma$) of the damping fluctuations γ. The robustness of GCF stems largely from its tendency to underestimates covariances when compared to SPEKF; for incorrect parameters SPEKF propagates the incorrect statistics more accurately which can lead to more spurious results.

Parameter estimation:

(1) SPEKF, GCF, and SDMF are comparable and skillful at estimating the mean values of the hidden stochastic parameters $\gamma(t)$ and $b(t)$.
(2) SPEKF is generally the best filter at recovering the dominant negative minima of $\gamma(t)$ even in cases where the damping fluctuations decorrelate rapidly compared to the observation time step. This feature also helps SPEKF improve its overall filtering skill. GCF and DMF are generally comparable to SPEKF for parameter estimation but they are somewhat less skillful at large observation time steps.
(3) TEKF and SDMF are completely unreliable at estimating the stochastic parameters in signals containing intermittent bursts of transient instability (regimes I and II). They often predict phases of strong stability in the filtered signal $u(t)$ during phases of transient instability in the truth, i.e., when $\gamma(t) < 0$.

We stress here that while the limited representation of model error assuming perfect model structure and uncertainties in the model parameters is appropriate for understanding the effects of incorrect statistics on the filter performance, the above filter hierarchy does not necessarily generalize to situations when a posteriori analysis of the forecast error variance can be carried out and the model covariance is inflated to minimize the innovation variance in order to reduce the forecast model error. However, the results presented here should provide useful guidelines for developing cheap, skillful and robust techniques for filtering spatially extended systems with multiple spatio-temporal scales in the presence of significant model error and sparse observations. Moreover, the robustness of SPEKF and GCF (using consistent moment closures) for real-time stochastic parameterization of the unresolved scales in the turbulent spectrum should prove valuable for developing more skillful superresolution techniques in geosciences (e.g. [35]), as well as for superparameterization methods in complex multi-scale systems [45,47] including eddy parameterization schemes for ocean climate models.

Acknowledgement

The research of A. Majda is partially supported by NFS grant DMS-0456713, NSF CMG grant DMS-1025468, and ONR grants ONR-DRI N00014-10-1-0554 and N00014-11-1-0306. M. Branicki and B. Gershgorin are supported as postdoctoral fellows on the last two grants.

Appendix A. Derivation of the exact criterion for mean-stable dynamics of the test model

We recapitulate here some exact analytical formulas for the path-wise solutions and the first moments of the system (1) which are necessary in deriving the mean-stability criterion (see (2) in Proposition 1). The complete set of analytical formulas for the second order statistics of (1) can be found in [21]. The proof of Proposition 1 is outlined at the end.

Path-wise solutions of the nonlinear model (1) are given by

$$b(t) = \hat{b} + (b_0 - \hat{b})e^{-\lambda_b(t-t_0)} + \sigma_b \int_{t_0}^{t} e^{-\lambda_b(t-s)} \mathrm{d}W_b(s), \tag{A.1}$$

$$\gamma(t) = \hat{\gamma} + (\gamma_0 - \hat{\gamma})e^{-d_\gamma(t-t_0)} + \sigma_\gamma \int_{t_0}^{t} e^{-d_\gamma(t-s)} \mathrm{d}W_\gamma(s), \tag{A.2}$$

$$u(t) = e^{-J(t_0,t)+\hat{\lambda}(t-t_0)}u_0 + \int_{t_0}^{t} (b(s) + f(s))e^{-J(s,t)+\hat{\lambda}(t-s)}\mathrm{d}s + \sigma_u \int_{t_0}^{t} e^{-J(s,t)+\hat{\lambda}(t-s)}\mathrm{d}W(s), \tag{A.3}$$

where b_0, γ_0, u_0 are the initial conditions at t_0 and

$$\lambda_b = -\gamma_b + i\omega_b, \quad \hat{\lambda} = -\hat{\gamma} + i\omega, \quad J(s,t) = \int_s^t (\gamma(s) - \hat{\gamma})\mathrm{d}s. \tag{A.4}$$

The mean of $u(t)$ is

$$\langle u(t)\rangle = (\langle u_0\rangle - Cov(u_0, J(t_0,t)))e^{\hat{\lambda}(t-t_0) - \langle J(t_0,t)\rangle + \frac{1}{2}Var(J(t_0,t))} + \int_{t_0}^{t} (\hat{b} + e^{\lambda_b(s-t_0)}(\langle b_0\rangle - \hat{b} - Cov(b_0, J(s,t))))e^{\hat{\lambda}(t-s) - \langle J(s,t)\rangle + \frac{1}{2}Var(J(s,t))}\mathrm{d}s + \int_{t_0}^{t} f(s)e^{\hat{\lambda}(t-s) - \langle J(s,t)\rangle + \frac{1}{2}Var(J(s,t))}\mathrm{d}s, \tag{A.5}$$

where

$$\langle J(s,t)\rangle = \frac{1}{d_\gamma^2}\left(e^{-d_\gamma(s-t_0)} - e^{-d_\gamma(t-t_0)}\right)(\langle\gamma_0\rangle - \hat{\gamma}), \tag{A.6}$$

$$Var(J(s,t)) = \frac{1}{d_\gamma^2}\left(e^{-d_\gamma(s-t_0)} - e^{-d_\gamma(t-t_0)}\right)Var(\gamma_0) - \frac{\sigma_\gamma^2}{d_\gamma^3}\left[1 + d_\gamma(s-t) + e^{-d_\gamma(s+t-2t_0)}\left(\cosh(d_\gamma(s-t)) - 1 - e^{2d_\gamma(s-t_0)}\right)\right], \tag{A.7}$$

and

$$Cov(u_0, J(s,t)) = \frac{1}{d_\gamma}\left(e^{-d_\gamma(s-t_0)} - e^{-d_\gamma(t-t_0)}\right)Cov(u_0, \gamma_0), \tag{A.8}$$

$$Cov(b_0, J(s,t)) = \frac{1}{d_\gamma}\left(e^{-d_\gamma(s-t_0)} - e^{-d_\gamma(t-t_0)}\right)Cov(b_0, \gamma_0). \tag{A.9}$$

The variance of $u(t)$ and all components of the covariance matrix are given in [21]. It is important to note that, due to the nonlinearity of (1), solutions with Gaussian initial statistics at $t = t_0$ will not remain Gaussian for $t > t_0$.

Proof of Proposition 1. We prove here Proposition 1 (cf. Section 2), which determines a condition for the mean-stability of the dynamics of the system (1). We first show that (2) is a necessary condition for the mean stability of the system (1). We then show that it is also sufficient.

Consider the first term in (A.5) given by

$$(\langle u_0\rangle - Cov(u_0, J(t_0,t)))e^{\hat{\lambda}(t-t_0) - \langle J(t_0,t)\rangle + \frac{1}{2}Var(J(t_0,t))}. \tag{A.10}$$

Assuming that the statistics at t_0 is bounded and $d_\gamma > 0$, the terms in the bracket in (A.10) are bounded on $[t_0, \infty)$ since $\langle u_0\rangle < \infty$ and, using (A.8), we have

$$\max_{t_0 \leqslant t < \infty} Cov(u_0, J(t_0,t)) = \frac{1}{d_\gamma} Cov(u_0, \gamma_0) < \infty. \tag{A.11}$$

It can be easily seen from (A.6) and (A.7) that the exponential term in (A.10) is bounded for any finite $t \geqslant t_0$ and it is also bounded on $[t_0, \infty)$ provided that

$$\lim_{t\to\infty} \Re e\left[\hat{\lambda}(t-t_0) - \langle J(t_0,t)\rangle + \frac{1}{2}Var(J(t_0,t))\right] < 0. \tag{A.12}$$

The condition (A.12) can be rewritten, using (A.6) and (A.7), as

$$\lim_{t\to\infty}\left\{-\hat{\gamma}(t-t_0) - \frac{1}{d_\gamma^2}(1 - e^{-d_\gamma(t-t_0)})\left(\langle\gamma_0\rangle - \hat{\gamma} + \frac{1}{2}Var(\gamma_0)\right) - \frac{\sigma_\gamma^2}{2d_\gamma^3}[1 - d_\gamma(t-t_0) + e^{-d_\gamma(t-t_0)}(\cosh(d_\gamma(t-t_0)) - 2)]\right\} < 0. \tag{A.13}$$

For $t \gg 1$, the terms in the brackets can be approximated as

$$\Re e\left[\hat{\lambda}(t-t_0) - \langle J(t_0,t)\rangle + \frac{1}{2}Var(J(t_0,t))\right] = \left(-\hat{\gamma} + \frac{\sigma_\gamma^2}{2d_\gamma^2}\right)t + \mathcal{O}(1). \tag{A.14}$$

Please cite this article in press as: M. Branicki et al., Filtering skill for turbulent signals for a suite of nonlinear and linear extended Kalman filters, J. Comput. Phys. (2011), doi:10.1016/j.jcp.2011.10.029

Clearly, the condition (A.12) is satisfied when

$$-\hat{\gamma}+\frac{\sigma_\gamma^2}{2d_\gamma^2}<0, \tag{A.15}$$

as claimed. Note that this condition cannot be satisfied when $\hat{\gamma}<0$.

We now show that the condition (A.15) is also sufficient for mean stability of the system (1). Consider the second part of (A.5) given by the integral

$$\int_{t_0}^{t}(\hat{b}+e^{\lambda_b(s-t_0)}(\langle b_0\rangle-\hat{b}-Cov(b_0,J(s,t))))e^{\hat{\lambda}(t-s)-\langle J(s,t)\rangle+\frac{1}{2}Var(J(s,t))}\mathrm{d}s, \tag{A.16}$$

and two functions $\mathcal{A}_1(t,t_0),\mathcal{A}_2(t,t_0)$ which are bounded on $[t_0,\infty)$ and given by

$$\mathcal{A}_1(t,t_0)=\max_{s\in[t_0,t]}|\hat{b}+e^{\lambda_b(s-t_0)}(\langle b_0\rangle-\hat{b}-Cov(b_0,J(s,t)))|, \tag{A.17}$$

and

$$\mathcal{A}_2(t,t_0)=\max_{s\in[t_0,t]}\Re e\left[-\langle J(s,t)\rangle+\frac{1}{2}Var(J(s,t))-\frac{\sigma^2}{2d_\gamma^2}(t-s)\right]. \tag{A.18}$$

Boundedness of these functions can be easily deduced from (A.6)–(A.9). In particular, we can use the following estimates (for $d_\gamma>0$)

$$\mathcal{A}_1(t,t_0)\leqslant\frac{1}{d_\gamma^2}|Var(\gamma_0)/2-\langle\gamma_0\rangle+\hat{\gamma}|+\frac{\sigma_\gamma^2}{2d_\gamma^3}, \tag{A.19}$$

and

$$\mathcal{A}_2(t,t_0)\leqslant|\hat{b}|+|\langle b_0\rangle|+\frac{1}{d_\gamma}|Cov(b_0,\gamma_0)|. \tag{A.20}$$

Using the functions $\mathcal{A}_1,\mathcal{A}_2$ and assuming that (A.15) holds, we obtain the following estimate

$$\begin{aligned}&\max_{t\in[t_0,\infty)}\left|\int_{t_0}^{t}(\hat{b}+e^{\lambda_b(s-t_0)}(\langle b_0\rangle-\hat{b}-Cov(b_0,J(s,t))))e^{\hat{\lambda}(t-s)-\langle J(s,t)\rangle+\frac{1}{2}Var(J(s,t))}\mathrm{d}s\right|\\&\leqslant\max_{t\in[t_0,\infty)}\left(\mathcal{A}_1(t,t_0)e^{\mathcal{A}_2(t,t_0)}\int_{t_0}^{t}e^{\left(-\hat{\gamma}+\frac{\sigma_\gamma^2}{2d_\gamma^2}\right)(t-s)}\mathrm{d}s\right)<\infty,\end{aligned} \tag{A.21}$$

where we use the fact that $|\int h(t,s)\mathrm{d}s|\leqslant\int|h(t,s)|\mathrm{d}s$. Analogous argument holds for the second integral in (A.5) as long as the (scalar) forcing remains bounded, i.e., there exists a constant C such that $\max_{t\in[t_0,\infty)}|f(t)|<C$. This completes the proof.

Appendix B. Details of filter implementations

B.1. Tangent EKF (TEKF)

This is the classical procedure of deriving the EKF in which the system (1) is linearized about the posterior mean at the previous observation time $(u_{m|m},b_{m|m},\gamma_{m|m})^T$, leading to a system for the expected value $\mathbf{U}^T=(\bar{u},\bar{b},\bar{\gamma})^T$ in the form

$$\frac{\mathrm{d}\mathbf{U}}{\mathrm{d}t}=L_{m|m}\mathbf{U}+\mathbf{\Phi}(t), \tag{B.1}$$

where

$$L_{m|m}=\begin{pmatrix}\lambda_{m|m}&1&-u_{m|m}\\0&\lambda_b&0\\0&0&-d_\gamma^M\end{pmatrix},\quad\lambda_{m|m}=-\gamma_{m|m}+i\omega_u^M,\lambda_b=-\gamma_b^M+i\omega_b^M, \tag{B.2}$$

and the inhomogeneity $\mathbf{\Phi}(t)=(f(t),0,0)^T$ represents the deterministic forcing.

The prior mean at the next time step $(\bar{u}_{m+1|m},\bar{b}_{m+1|m},\bar{\gamma}_{m+1|m})^T$ is obtained by integrating (B.1) between successive observation times with initial condition

$$(\bar{u}(t_m),\bar{b}(t_m),\bar{\gamma}(t_m))^T=(\bar{u}_{m|m},\bar{b}_{m|m},\bar{\gamma}_{m|m})^T,$$

Please cite this article in press as: M. Branicki et al., Filtering skill for turbulent signals for a suite of nonlinear and linear extended Kalman filters, J. Comput. Phys. (2011), doi:10.1016/j.jcp.2011.10.029

which leads to

$$\begin{pmatrix} \bar{u}_{m+1|m} \\ \bar{b}_{m+1|m} \\ \bar{\gamma}_{m+1|m} \end{pmatrix} = \begin{pmatrix} e^{\lambda_{m|m}\Delta t} & \frac{e^{\lambda_b \Delta t} - e^{\lambda \Delta t}}{\lambda_b - \lambda_{m|m}} & -u_{m|m} \frac{e^{\lambda \Delta t} - e^{-d_\gamma \Delta t}}{d_\gamma - \lambda_{m|m}} \\ 0 & e^{\lambda_b \Delta t} & 0 \\ 0 & 0 & e^{-d_\gamma \Delta t} \end{pmatrix} \begin{pmatrix} \bar{u}_{m|m} \\ \bar{b}_{m|m} \\ \bar{\gamma}_{m|m} \end{pmatrix} + \begin{pmatrix} \tilde{f} \\ 0 \\ 0 \end{pmatrix} \tag{B.3}$$

where

$$\tilde{f} = \int_{t_m}^{t_{m+1}} f(s) e^{\lambda_{m|m}(t_{m+1}-s)} \mathrm{d}s. \tag{B.4}$$

The covariance is updated in the same way as in SDMF using the linear Eq. (B.1) with the Jacobian $L_{m|m}$ rewritten in real variables and integrated between successive observation times, leading to

$$R_{m+1|m} = e^{A_{m|m}\Delta t} R_{m|m} e^{A_{m|m}^T \Delta t} + \int_{t_m}^{t_{m+1}} e^{A_{m|m}(t_{m+1}-s)} \Sigma e^{A_{m|m}^T (t_{m+1}-s)} \mathrm{d}s. \tag{B.5}$$

B.2. Deterministic Mean Filter (DMF)

This filter is commonly known in engineering literature as the continuous discrete extended Kalman filter. Following the derivation in Section 3, the mean $(\bar{u}, \bar{b}, \bar{\gamma})$ and covariance matrix

$$R(t) = \begin{pmatrix} u' \\ b' \\ \gamma' \end{pmatrix} \cdot (u', b', \gamma') \tag{B.6}$$

in DMF is propagated using

$$\begin{cases} (a) & \dot{\bar{u}}(t) = (-\bar{\gamma}(t) + i\omega_u^M)\bar{u}(t) + \bar{b}(t) + f(t), \\ (b) & \dot{\bar{b}}(t) = (-\gamma_b^M + i\omega_b^M)(\bar{b}(t) - \hat{b}^M), \\ (c) & \dot{\bar{\gamma}}(t) = -d_\gamma^M(\bar{\gamma}(t) - \hat{\gamma}^M), \\ (d) & \dot{R}(t) = A(\bar{u}, \bar{b}, \bar{\gamma})R(t) + R(t)A(\bar{u}, \bar{b}, \bar{\gamma})^T + \Sigma, \end{cases} \tag{B.7}$$

where A is the Jacobian of (1)

$$A(\bar{u}(t), \bar{b}(t), \bar{\gamma}(t)) = \begin{pmatrix} -\bar{\gamma}(t) & -\omega^M & 1 & 0 & -\Re e[\bar{u}(t)] \\ \omega^M & -\bar{\gamma}(t) & 0 & 1 & -\Im m[\bar{u}(t)] \\ 0 & 0 & -\gamma_b^M & -\omega_b^M & 0 \\ 0 & 0 & \omega_b^M & -\gamma_b^M & 0 \\ 0 & 0 & 0 & 0 & -d_\gamma^M \end{pmatrix}, \tag{B.8}$$

which is evaluated at the current state, $(\bar{u}, \bar{b}, \bar{\gamma})^T$, of the system (B.7), and $\Sigma \equiv \mathrm{diag}\left[\left(\frac{1}{2}\left((\sigma_u^M)^2, \frac{1}{2}(\sigma_u^M)^2, \frac{1}{2}(\sigma_b^M)^2, \frac{1}{2}(\sigma_b^M)^2, \left(\sigma_\gamma^M\right)^2\right)\right)\right]$.

B.3. Split Deterministic Mean Filter (SDMF)

In this filter the prior mean and covariance are updated separately. Here the mean is updated first by solving (B.7a-c) on a time interval $[t_m, t_{m+1}]$ with initial condition given by the posterior mean at t_m, i.e., $(\bar{u}(t_m), \bar{b}(t_m), \bar{\gamma}(t_m))^T = (\bar{u}_{m|m}, \bar{b}_{m|m}, \bar{\gamma}_{m|m})^T$.

The covariance is updated using the linear Eq. (B.7) with the Jacobian A evaluated at the posterior mean, i.e., $A(t_m) = A_{m|m}$, and integrated between successive observation times, leading to

$$R_{m+1|m} = e^{A_{m|m}\Delta t} R_{m|m} e^{A_{m|m}^T \Delta t} + \int_{t_m}^{t_{m+1}} e^{A_{m|m}(t_{m+1}-s)} \Sigma e^{A_{m|m}^T (t_{m+1}-s)} \mathrm{d}s. \tag{B.9}$$

B.4. Gaussian Closure Filter (GCF)

In a Gaussian Closure Filter the prior statistics is propagated using a nonlinear dynamical system which is obtained by neglecting third and higher moments in the probability distribution associated with the system (1). The posterior update is carried out using the steps (8)–(10) as in the other filters. The second-order statistics can be obtained directly from the system (16) by substituting (1) for $\boldsymbol{f}(\boldsymbol{x}, t)$. Here, we sketch an alternative derivation specific to the system (1).

Please cite this article in press as: M. Branicki et al., Filtering skill for turbulent signals for a suite of nonlinear and linear extended Kalman filters, J. Comput. Phys. (2011), doi:10.1016/j.jcp.2011.10.029

Given the system (1), we use the average Reynolds decomposition to represent all variables in (1) as the sum of a mean and fluctuations around the mean, i.e.,

$$u = \bar{u} + u', \quad b = \bar{b} + b', \quad \gamma = \bar{\gamma} + \gamma', \tag{B.10}$$

$$\langle u \rangle = \bar{u}, \langle b \rangle = \bar{b}, \langle \gamma \rangle = \bar{\gamma}, \langle u' \rangle = 0, \langle b' \rangle = 0, \langle \gamma' \rangle = 0. \tag{B.11}$$

The equations for the mean and fluctuations can be easily obtained from (1) and (B.10)-(B.11) in the form

$$\mathrm{d}\bar{u} = [(-\bar{\gamma} + i\omega)\bar{u} - \overline{u'\gamma'} + \bar{b} + f]\mathrm{d}t, \tag{B.12}$$

$$\mathrm{d}u' = [(-\bar{\gamma} + i\omega)u' + b' - \bar{u}\gamma' - u'\bar{\gamma} + \overline{u'\gamma'}]\mathrm{d}t + \sigma_u \mathrm{d}W_u, \tag{B.13}$$

$$\mathrm{d}\bar{b} = (-\gamma_b + i\omega_b)(\bar{b} - \hat{b})\mathrm{d}t, \quad \mathrm{d}b' = (-\gamma_b + i\omega_b)b'\mathrm{d}t + \sigma_b \mathrm{d}W_b, \tag{B.14}$$

$$\mathrm{d}\bar{\gamma} = -d_\gamma(\bar{\gamma} - \hat{\gamma})\mathrm{d}t, \mathrm{d}\gamma' = -d_\gamma\gamma'\mathrm{d}t + \sigma_\gamma \mathrm{d}W_\gamma. \tag{B.15}$$

A closed twelve-dimensional dynamical system for the first and second moments,

$$\bar{u}, \bar{b}, \bar{\gamma}, \quad \overline{|u'|^2}, \overline{u'^2}, \overline{|b'|^2}, \overline{b'^2}, \overline{\gamma'^2}, \quad \overline{u'b'}, \overline{u'b'^*}, \overline{u'\gamma'}, \overline{b'\gamma'}, \tag{B.16}$$

which are needed in the Kalman filter can be found using (B.12)–(B.15) and the multivariate Ito formula (e.g., [19]) and assuming the Gaussian closure (i.e., $E[(X - E(X))^p] = 0$, where p odd).

As an example, consider the evolution of $|u'|^2$ which can be derived using the Ito formula and (B.13) as

$$\mathrm{d}\overline{|u'|^2} = \left[-2\bar{\gamma}\overline{|u'|^2} + \overline{u'b'^*} + \overline{u'^*b'} - \bar{u}\overline{u'^*\gamma'} - \bar{u}^*\overline{u'\gamma'} - 2\overline{|u'|^2\gamma'} + \sigma_u^2\right]\mathrm{d}t. \tag{B.17}$$

Following the Gaussian closure approximation, we assume that the third moment, $\overline{|u'|^2\gamma'}$, in (B.17) vanishes. Consequently, the resulting approximation leads to

$$\mathrm{d}\overline{|u'|^2} \approx \left[-2\bar{\gamma}\overline{|u'|^2} + \overline{u'b'^*} + \overline{u'^*b'} - \bar{u}\overline{u'^*\gamma'} - \bar{u}^*\overline{u'\gamma'} + \sigma_u^2\right]\mathrm{d}t. \tag{B.18}$$

Similar procedure leads to dynamical equations for all the variables (B.16).

References

[1] J. Anderson, An ensemble adjustment Kalman filter for data assimilation, Mon. Wea. Rev. 129 (2001) 2884–2903.
[2] J. Anderson, A local least squares framework for ensemble filtering, Mon. Wea. Rev. 131 (2003) 634–642.
[3] J. Anderson, Spatially and temporally varying adaptive covariance inflation for ensemble filters, Tellus A 61 (1) (2009) 72–83.
[4] A. Bain, D. Crisan, Fundamentals of Stochastic Filtering, Springer, New York, 2009.
[5] S.-J. Baek, B.R. Hunt, E. Kalnay, E. Ott, I. Szunyogh, Local ensemble Kalman filtering in the presence of model bias, Tellus 58A (2006) 293–306.
[6] T. Bengtsson, P. Bickel, B. Li, Curse of dimensionailty revisited: Collapse of the particle filter in very large scale systems, in: D. Nolan, T. Speed (Eds.), IMS Lecture Notes – Monograph Series in Probability and Statistics: Essays in Honor of David A. Freedman, vol. 2, Institute of Mathematical Sciences, 2008, pp. 316–334.
[7] P. Bickel, B. Li, T. Bengtsson, Sharp failure rates for the bootstrap filter in high dimensions, in IMS Lecture Notes – Monograph Series: Essays in Honor of J.K. Gosh, Institute of Mathematical Sciences (2008) 318–329.
[8] C. Bishop, B. Etherton, S. Majumdar, Adaptive sampling with the ensemble transform Kalman filter Part I: The theoretical aspects, Mon. Wea. Rev. 129 (2001) 420–436.
[9] R. Buizza, M. Miller, T.N. Palmer, Stochastic representation of model uncertainties in the ECMWF ensemble prediction system, Q. J. R. Meteorol. Soc. 125 (1999) 2887–2908.
[10] A. Chorin, P. Krause, Dimensional reduction for a Bayesian filter, PNAS 101 (2004) 15013–15017.
[11] S.E. Cohn, An introduction to estimation theory, J. Meteor. Soc. Jpn. 75 (1997) 257–288.
[12] J.L. Crassidis, F.L. Markley, Unscented filtering for spacecraft attitude estimation, J. Guid. Control Dyn. 26 (2003) 536–542.
[13] T. Delsole, Stochastic model of quasigeostrophic turbulence, Surv. Geophys. 25 (2) (2004) 107–149.
[14] G. Evensen, Using the extended Kalman filter with a multilayer quasi-geostrophic ocean model, J. Geophys. Res. 97 (C11) (1992) 17905–17924.
[15] G. Evensen, The ensemble Kalman filter: Theoretical formulation and practical implementation, Ocean Dyn. 53 (2003) 343–367.
[16] B. Farrell, P. Ioannou, State estimation using a reduced-order Kalman filter, J. Atmos. Sci. 58 (2001) 3666–3680.
[17] B. Friedland, Treatment of bias in recursive filtering, IEEE Trans. Autom. Control AC-14 (1969) 359–367.
[18] B. Friedland, Estimating sudden changes of biases in linear dynamical systems, IEEE Trans. Autom. Control AC-27 (1982) 237–240.
[19] C. Gardiner, Handbook of Stochastic Methods for Physics, Chemistry, and the Natural Sciences, Springer-Verlag, 1997.
[20] A. Gelb, Applied optimal estimation, The M.I.T. Press, Cambridge, 1988.
[21] B. Gershgorin, J. Harlim, A.J. Majda, Test models for improving filtering with model errors through stochastic parameter estimation, J. Comput. Phys 229 (1) (2010) 1–31.
[22] B. Gershgorin, J. Harlim, A.J. Majda, Improving filtering and prediction of spatially extended turbulent systems with model errors through stochastic parameter estimation, J. Comput. Phys 229 (2010) 32–57.
[23] B. Gershgorin, A.J. Majda, A nonlinear test model for filtering slow-fast systems, Commun. Math. Sci. 6 (2008) 611–649.
[24] B. Gershgorin, A.J. Majda, Filtering a nonlinear slow-fast system with strong fast forcing, Commun. Math. Sci. 8 (2009) 67–92.
[25] B. Gershgorin, A.J. Majda, Filtering a Statistically Exactly Solvable Test Model for Turbulent Tracers from Partial Observations, J. Comput. Phys. 230 (4) (2011) 1602–1638.
[26] M. Ghil, P. Malanotte-Rizolli, Data assimilation in meteorology and oceanography, Adv. Geophys. 33 (1991) 141–266.
[27] J. Harlim, A. Majda, Filtering turbulent sparsely observed geophysical flows, Mon. Wea. Rev. 138 (4) (2010) 1050–1083.
[28] K. Haven, A.J. Majda, R. Abramov, Quantifying predictability through information theory: Small sample estimation in a non-gaussian framework, J. Comput. Phys. 206 (2005) 334–362.
[29] B. Hunt, E. Kostelich, I. Szunyogh, Efficient data assimilation for spatiotemporal chaos: A local ensemble transform Kalman filter, Phys. D 230 (2007) 112–126.
[30] A.H. Jazwinski, Stochastic processes and filtering theory, Academic Press, New York, 1970.

Please cite this article in press as: M. Branicki et al., Filtering skill for turbulent signals for a suite of nonlinear and linear extended Kalman filters, J. Comput. Phys. (2011), doi:10.1016/j.jcp.2011.10.029

[31] K. Judd, T. Stemler, Failures of sequential Bayesian filters and the successes of shadowing filters in tracking of nonlinear deterministic and stochastic systems, Phys. Rev. E 79 (2009) 066206.
[32] R.E. Kalman, A new approach to linear filtering and prediction problems, J. Basic Eng. (Ser. D) 82 (1960) 35–45.
[33] R.E. Kalman, R.S. Bucy, New results in linear filtering and prediction problems, J. Basic Eng. (ASME) 83D (1961).
[34] E. Kalnay, Atmospheric Modeling, Data Assimilation and Predictability, Cambridge University Press, 2003.
[35] S.R. Keating, A.J. Majda, K.S. Smith, New methods for estimating poleward eddy heat transport using satellite altimetry, J. Phys. Oceanogr., accepted for publication.
[36] E.J. Lefferts, F.L. Markley, M.D. Shuster, Kalman filtering for spacecraft attitude estimation, J. Guidance, Control, Dyn. 5 (1982) 417–429.
[37] G. Leu, R. Baratti, An extended Kalman filtering approach with a criterion to set its tuning parameters; application to a catalytic reactor, Comput. Chem. Eng. 23 (2000) 1839–1849.
[38] P. van Leeuwen, Particle filtering in geosciences, Mon. Wea. Rev. 137 (2009) 4089–4114.
[39] A.J. Majda, R.V. Abramov, M.J. Grote, Information theory and stochastics for multiscale nonlinear systems, CRM Monogr. Ser., vol. 25, American Mathematical Society, Providence, Rhode Island, USA, 2005.
[40] A.J. Majda, M.J. Grote, Explicit off-line criteria for stable accurate time filtering of strongly unstable spatially extended systems, PNAS 104 (2007) 1124–1129.
[41] A.J. Majda, J. Harlim, B. Gershgorin, Mathematical strategies for filtering turbulent dynamical systems, DC DS 27 (2) (2010) 441–486.
[42] A.J. Majda, I. Timofeyev, E. Vanden-Eijnden, Models for stochastic climate prediction, Proc. Nat. Acad. Sci. 96 (1999) 15687–15691.
[43] A.J. Majda, I. Timofeyev, E. Vanden-Eijnden, Systematic strategies for stochastic mode reduction in climate, J. Atmos. Sci. 60 (2003) 1705–1722.
[44] A.J. Majda, I. Timofeyev, Low dimensional chaotic dynamics versus intrinsic stochastic chaos: A paradigm model, Phys. D 199 (2004) 339–368.
[45] A.J. Majda, Multiscale models with moisture and systematic strategies for superparameterization, J. Atmos. Sci. 64 (2007) 2726–2734.
[46] A.J. Majda, C. Franzke, B. Khouider, An applied mathematics perspective on stochastic model ling for climate, Phil. Trans. A 366 (2008) 2429–2455.
[47] A.J. Majda, M. Grote, Mathematical test models for superparameterization in anisotropic turbulence, Proc. Nat. Acad. Sci. USA 106 (14) (2009) 5470–5474.
[48] A.J. Majda, J. Harlim, Filtering Turbulent Signals in Complex Systems, Cambridge University Press, UK, 2011.
[49] P.D. Moral, Nonlinear filtering: Interacting particle solutions, Markov Processes and Related Fields 2 (1996) 555–580.
[50] P.D. Moral, J. Jacod, Interacting particle filtering with discrete observation, in: Sequential Monte-Carlo Methods in Practice Volume, in: Doucet A., de Freitas N., Gordon N. (Eds.), Statistics for Engineering and Information Science, Springer, 2001, pp. 43–75.
[51] T.N. Palmer, G.J. Shutts, R. Hagedorn, F.J. Doblas-Reyes, T. Jung, M. Leutbecher, Representing Model Uncertainty in Weather and Climate Prediction, Annu. Rev. Earth Planet. Sci 33 (2005) 163–193.
[52] W.H. Ray, Advanced Process Control, McGraw Hill, New York, 1981.
[53] B.J. Rye, R.M. Hardesty, Nonlinear Kalman filtering techniques for incoherent backscatter lidar: return power and log power estimation, Appl. Optics. 28 (18) (1989) 3908–3917.
[54] X. Sun, L. Jin, M. Xiong, Extended Kalman Filter for Estimation of Parameters in Nonlinear State-Space Models of Biochemical Networks. PLoS ONE 3 (11) (2008) e3758, doi:10.1371/journal.pone.0003758.
[55] T.J. Slight, C.N. Ironside, C.R. Stanley, M. Hopkinson, C.D. Farmer, Integration of a resonant tunneling diode and optical communications laser, IEEE Photon. Tech. Lett. 18 (14) (2006) 1518–1520.
[56] Ch. Snyder, T. Bengtsson, P. Bickel, J. Anderson, Obstacles to High-dimensional Particle Filtering, Mon. Wea. Rev. 136 (2008) 4629–4640.
[57] I. Szunyogh, E.G. Kostelich, D. Gyarmati, B. Patil, E. Hunt, E. Kalnay, Ott, J. Yorke, Assessing a local ensemble Kalman filter: Perfect model experiments with the NCEP global model, Tellus A, 57 2005, pp. 528–545.
[58] R. Todling, M. Ghil, Tracking atmospheric instabilities with the Kalman filter. Part I: Methodology and one-layer results, Mon. Wea. Rev. 122 (1994) 183–204.
[59] J.J. Tribbia, D.P. Baumhefner, The reliability of improvements in deterministic short-range forecasts in the presence of initial state and modeling deficiencies, Mon. Wea. Rev. 116 (1988) 2276–2288.
[60] Xiong Kai, Liu Liangdong, Liu Yiwu, Robust extended Kalman filtering for nonlinear systems with multiplicative noises, Optim. Control Appl. Meth. 32 (2011) 47–63.
[61] G. Valverde, V. Terzija, Unscented kalman filter for power system dynamic state estimation, Generation, Transmission & Distribution, IET 5 (1) (2011) 29–37, doi:10.1049/iet-gtd.2010.0210.
[62] S. Zerouali, A. Allag, S.M. Mimoune, K. Srairi, A.H. Hamida, M. Féliachi, Extended Kalman filter for uninterruptible power supplies applied to non linear loads, Int. J. Appl. Electromag. Mech. 25 (2007) 565–569.

Please cite this article in press as: M. Branicki et al., Filtering skill for turbulent signals for a suite of nonlinear and linear extended Kalman filters, J. Comput. Phys. (2011), doi:10.1016/j.jcp.2011.10.029